

**Development of Interdigitated Electrode Sensors for Monitoring the  
Dielectric Properties of Lubricant Oils**

by

Jacob Wade Craft

A thesis submitted to the Graduate Faculty of  
Auburn University  
in partial fulfillment of the  
requirements for the Degree of  
Master of Science

Auburn, Alabama  
December 13, 2010

Copyright 2010 by Jacob Wade Craft

Approved by

Dong-Joo Kim, Chair, Associate Professor of Materials Engineering  
Jeffrey Fergus, Professor of Materials Engineering  
Barton Prorok, Associate Professor of Materials Engineering

## Abstract

Proper lubrication is a necessary step in protecting the engine of any vehicle. Regular changing of the lubricating oil becomes an important part of keeping the vehicle running for an extended life. Currently, lubricant oil is changed based on a scheduled time frame or set mileage. It would be advantageous, however, to be able to detect the properties of oil and tell when lubricant change is necessary to reduce waste and excess cost.

The goal of this research is to develop and optimize an IDT sensor to measure the change in the capacitance value of lubricant oil. To optimize the sensor, four design parameters were chosen and varied between several series of IDT electrodes. The electrodes were fabricated and tested to observe how each of the parameters, electrode width, finger thickness, finger spacing and number of fingers, would affect the sensitivity of the capacitance measurements. Several trends of how they affect the sensitivity were observed and the relative importance of each factor was determined. In general, a maximization of the sensing area by increasing electrode width and finger thickness was the most influential. The spacing of the electrode fingers is also a very important factor though the biggest changes are only seen at very small spacing's. The effect of substrate material was also studied and was found to have some effect.

## Acknowledgments

I would like to thank Dr. Kim and the members of my committee, Dr. Fergus and Dr. Prorok for all of their help and guidance. I would also like to thank my group members, Dr. Wikle, L.C. Mathison, Joshua, Dan, Ho Sang, Seon Bae and Ishita for their help and support. Finally, I would like to thank my friends and my family for their love and support throughout this process.

## Table of Contents

Abstract .....	ii
Acknowledgments.....	iii
List of Tables .....	vi
List of Figures .....	vii
List of Abbreviations .....	ix
Chapter 1 Introduction .....	1
1.1 Overview .....	1
1.2 Thesis Structure .....	2
Chapter 2 General Background.....	3
2.1 Oil Degradation and Current Testing Methods.....	3
2.1.1 Oil Degradation.....	3
2.1.2 Current Testing Methods .....	5
2.1.3 Current Research.....	7
2.1.4 Commercially Available Sensor Systems .....	17
2.2 Capacitance Sensors.....	18
2.2.1 General Principles .....	18
2.2.2 IDT Structure .....	19
2.2.3 IDC Model .....	21
Chapter 3 Experimental Setup and Techniques .....	25

3.1 Artificial Aging of Oil Samples .....	25
3.2 Fabrication of Sensors.....	28
3.3 Measurements .....	30
Chapter 4 Results and Discussion.....	32
4.1 Capacitance Measurements.....	33
4.1.1 Effect of IDT Geometry.....	33
4.1.2 Effect of Substrate Material .....	55
4.2 Optimization of Sensor .....	55
Chapter 5 Conclusions and Future Studies .....	57
References .....	59

## List of Tables

Table 2.1 ASTM standard test methods for determining the condition of lubricant oils .....	7
Table 2.2 Equations needed for calculation of $C_I$ and $C_E$ for finite and infinite layers. ....	24
Table 3.1 Data for BP turbo oil 2380.....	26
Table 3.2 Sputter Conditions for Metal Depositions .....	30
Table 4.1 Design parameters for Original IDT electrodes .....	33
Table 4.2 Design parameters for the second set of IDT electrodes. ....	36
Table 4.3 Design parameters for the final IDT electrode design. ....	42
Table 4.4 Effect of design factors on capacitance measurements. ....	52
Table 4.5 Capacitance per unit area for the 2 <sup>nd</sup> electrode series .....	54
Table 4.6 Capacitance per unit area for the 3 <sup>rd</sup> electrode series .....	54

## List of Figures

Figure 2.1 Reaction scheme for oxidation-polymerization reaction sequence .....	5
Figure 2.2 Lubricating oil viscosity vs. dielectric constant .....	8
Figure 2.3 Change of dielectric constants with temperature of fresh oil .....	9
Figure 2.4 Correlation between the measured dielectric constant and the sensing capacitance. ....	10
Figure 2.5 Characteristics of dielectric constant vs. temperature for engine oil.....	11
Figure 2.6 Dielectric constant vs. driving distance and its variance with temperature .....	11
Figure 2.7 Measured Dielectric Constant for grid capacitance sensor in various media.....	12
Figure 2.8 Change in the dielectric constant with different concentrations of contaminant particles. ....	13
Figure 2.9 Relationship between permittivity (Dielectric Constant) and acid number .....	14
Figure 2.10 Relationship between permittivity (Dielectric Constant) and iron content .....	15
Figure 2.11 Relationship between permittivity (Dielectric Constant) and moisture content .....	15
Figure 2.12 Relative dielectric constant variation of different polluted oil samples from fresh oil sample.....	16
Figure 2.13 Illustration of Delphi Oil Quality Sensor .....	18
Figure 2.14 Schematic diagram of an interdigitated electrode. ....	20
Figure 2.15 Plot of Calculated Capacitance vs. Finger spacing using equation 2.1 .....	21
Figure 2.16 (a) Layout of electrode (b) Cross section of electrode. ....	22
Figure 2.17 Equivalent circuit for IDC model. ....	22
Figure 3.1 Schematic diagram of the oil degradation vessel. ....	27

Figure 3.2 Photo of the oil degradation vessel. ....	27
Figure 3.3 Schematic of Fabrication Process.....	29
Figure 4.1 Capacitance vs. Frequency curve for 40s electrode .....	34
Figure 4.2 Capacitance vs. Frequency curve for 60s electrode .....	34
Figure 4.3 Capacitance vs. Frequency curve for 80s electrode .....	35
Figure 4.4 Capacitance vs. Frequency curve for 100s electrode .....	35
Figure 4.5 Capacitance vs. Frequency curve for T4S6F3 electrode .....	37
Figure 4.6 Capacitance vs. Frequency curve for T4S6F6 electrode. ....	37
Figure 4.7 Capacitance vs. Frequency curve for T4S6F9 electrode. ....	38
Figure 4.8 Capacitance vs. Frequency curve for T4S6F6L electrode.....	38
Figure 4.9 Change in capacitance vs. finger spacing.....	39
Figure 4.10 Plot of number of fingers vs. the change in capacitance. ....	40
Figure 4.11 Plot of change in capacitance vs. the electrode width. ....	40
Figure 4.12 Finger thickness vs. Change in capacitance. ....	41
Figure 4.13 Capacitance vs. Frequency curve for T2S5F6 Electrode .....	43
Figure 4.14 Capacitance vs. Frequency curve for T2S10F6 Electrode .....	44
Figure 4.15 Capacitance vs. Frequency curve for T4S5F6 Electrode .....	45
Figure 4.16 Capacitance vs. Frequency curve for T4S10F6 Electrode .....	46
Figure 4.17 Capacitance vs. Frequency curve for T4S10F6L Electrode .....	47
Figure 4.18 Comparison between measured value and the various models used. ....	49
Figure 4.19 Change in capacitance vs. Finger Width .....	50
Figure 4.20 Change in capacitance vs. Finger spacing .....	50
Figure 4.21 Change in capacitance vs. Electrode Width .....	51

## List of Abbreviations

IDT	Interdigitated Transducer
IDC	Interdigitated Capacitor
TAN	Total Acid Number
TBN	Total Base Number
ASTM	American Society for Testing and Materials
GPC	Gel Permeation Chromatography
FTIR	Fourier Transform Infrared Spectroscopy

# CHAPTER 1

## INTRODUCTION

### 1.1 Overview

Proper lubrication is a necessary step in protecting the engine of any vehicle. Regular changing of the lubricating oil becomes an important part of keeping the vehicle running for an extended life. Currently, most engine manufacturers recommend a scheduled approach to changing the engine lubricant. This scheduled maintenance is an effective way of making sure that the engine stays properly lubricated but can lead to wastefulness if the lubricant is changed before it is necessary. Condition based maintenance and oil changes would be preferable. It allows the engine lubricant to be changed only when needed and would save on maintenance costs in the long run.

With this in mind, a sensor to monitor the condition of the lubricant in situ has been studied. By using an interdigitated electrode structure as a capacitance sensor, the change in the capacitance value of oil with its degradation can be monitored. By determining at what point the lubricant becomes unfavorable for use in vehicle the engine lubricant can be changed at a point in time when it is necessary and save on maintenance costs.

The goal of the research is to study and develop this sensor to be implemented in the field. The theory behind how the sensor works is relatively simple and the main challenges were to determine how the geometrical and other parameters of the sensor affect the response and how to optimize the sensor for increased performance in the field. The geometry of the sensor used

has a large effect on the sensitivity of the device as well as the type of substrate material used in fabrication.

## **1.2 Thesis Structure**

Chapter 2 includes a literature survey from which this thesis work is based. The chemical degradation of oil based lubricants is discussed as well as general information on capacitance sensors and interdigitated electrodes.

Chapter 3 discusses the fabrication process for the sensors as well as the testing procedures for the finished products.

Chapters 4 and 5 present the results of the research and a discussion of the findings as well as a summary of the work and conclusions.

## CHAPTER 2

### GENERAL BACKGROUND

#### **2.1 Oil Degradation and Current Testing Methods**

Lubrication is an essential part of any type of machinery. One of the major types of lubricants in use currently is polyol ester based synthetic lubricants. The degradation and oxidation of these lubricants are of major concern to ensure that machinery stays properly lubricated with timely lubricant changes. In this section, the types of degradation that lubricants undergo and different methods of characterizing and analyzing that degradation will be discussed.

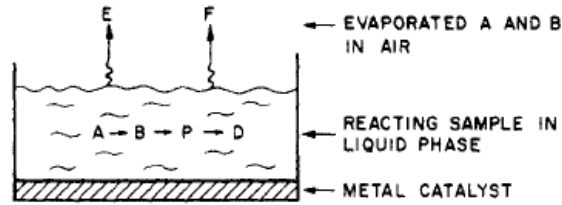
##### 2.1.1 Oil Degradation

The degradation of polyol ester based lubricants involves a complex series of reactions that have been the subject of much study.<sup>[1-5]</sup> When exposed to oxygen at high temperatures (over 200°C), lubricant oils will undergo a series of free radical chain reactions. Three major events occur in the breakdown: evaporation, oxidation and thermal degradation. The most influential of these is the oxidation reaction which is what causes the sludge and varnish build up that is detrimental to the effectiveness of the lubrication.<sup>[3,5]</sup>

All lubricant oils consist of long chain hydrocarbons that are susceptible to oxidation. Most engine oil manufacturers take this into account and use oxidation inhibitors in their products which will protect the lubricant from oxidation for some time and prolong its useful

life. However, when exposed to sufficient heat these oxidation inhibitors become unable to protect against the hydrocarbon chains becoming oxidized. The first step in the oxidation reaction for these oils is a free-radical chain reaction that will result in the production of hydroperoxides which will decrease the effectiveness of the lubricant. The hydroperoxides are unstable, however, and will convert to acids and ketones leading to an increased acid content in the oil. The products from the initial oxidation reactions that are now present in the lubricant are of low molecular weight. These byproducts will generally do one of two things; either evaporate into the gas phase or polymerize and form the high molecular weight products that are the cause of the increased viscosity of degraded oil and of the sludge and varnish deposits that are detrimental to the machinery in which the lubricant is being employed.<sup>[3,5]</sup>

Figure 2.1 shows the basic reaction scheme for the oxidation and polymerization of lubricant oil. As the oil is used part of it is lost to evaporation and part is oxidized into the low molecular weight liquid phase oxidation products. Again, some of these low molecular weight products will evaporate and the rest will polymerize into the high molecular weight liquid phase products. Finally, the high molecular weight products will continue to polymerize and eventually form as sludge and varnish on surfaces they are supposed to be lubricating.<sup>[3,5]</sup>



- A : ORIGINAL OIL
- B : LMW LIQUID PHASE OXIDATION PRODUCTS
- P : HMW LIQUID PHASE CONDENSATION POLYMERIZATION PRODUCTS
- D : SLUDGE AND VARNISH DEPOSITS
- E : EVAPORATED ORIGINAL OIL (A) IN THE VAPOR PHASE
- F : EVAPORATED LMW PRODUCTS (B) IN THE VAPOR PHASE

Figure 2.1 Reaction scheme for oxidation-polymerization reaction sequence.<sup>[3]</sup>

### 2.1.2 Current Testing Methods

There are many methods in use currently to monitor the condition of used oil once a sample has been taken from the vehicle. In this section some of the more prominent methods will be discussed along with the underlying principles that make the methods a useful indicator of the remaining useful life of the lubricant.

The first and most obvious test to run on a sample of lubricant oil is to measure its viscosity. The viscosity can be tested in a number of ways outlined by ASTM standards. The viscosity of the oil will tell a great deal about how much degradation has occurred. A fresh oil sample will usually be a light color and have a lower viscosity to aid in the lubrication and wetting of parts inside of the engine or machinery. An oil sample taken from an engine that has been used extensively will be dark and much thicker. This increase in viscosity is a result of the polymerization of the oxidation byproducts. The low molecular weight byproducts react and form long chain molecules with high molecular weights that can eventually become sludge and varnish deposits if allowed to react for too long.<sup>[3,5]</sup> The change in viscosity is the most

immediately apparent from a visual standpoint and is useful to determine if further testing is necessary.

Another valuable test that is often performed is the determination of the total acid number (TAN) or the total base number (TBN). These tests determine the pH of the oil which is very telling as to the amount of degradation that has taken place. As the oil oxidizes, the hydroperoxides that are formed are converted into acids which will raise the pH level of the oil.<sup>[3,5]</sup> As the degradation increases the TAN will increase and be a very good indicator of the amount of useful life that remains in the oil sample.

Another less commonly used method is gel permeation chromatography (GPC). GPC is most often used to determine the molecular weights of the byproducts of the degraded oil. As a sample is degraded, the byproducts will contain products with lower molecular weights, products with the same molecular weight, and products with high molecular weight. The GPC separates and collects data on the amounts of each present. An increase in the high molecular weight products will indicate a rise in the viscosity and a decrease in the lubrication potential of the oil.<sup>[2]</sup>

Various types of spectroscopy have been utilized in lubricant characterization as well including: visible, UV, infrared, and Fourier transformation infrared (FTIR). The spectroscopic techniques are easy ways to determine the amount of degradation of a sample in a short amount of time. Different peaks in these spectra relate to types of bonds that exist in the sample. By monitoring how the peaks change, a determination can be made as to what is taking place in the sample.<sup>[6]</sup>

Table 2.1 shows a summary of the common ASTM standard tests that can be performed on a lubricant oil to help to determine its condition. Some or all may be used to gather enough

information to determine if the oil is still useable. These tests are used to detect the amount of water in the oil, its TAN and TBN, its viscosity and color and the presence of wear metals and other contaminants. These are the type of tests that a commercial company would perform in a standard oil analysis.

Table 2.1 ASTM standard test methods for determining the condition of lubricant oils.

<b><i>Standard</i></b>	<b><i>Description</i></b>
ASTM D 4377	<i>Standard Test Method for Water in Crude Oils by Potentiometric Karl Fischer Titration</i>
ASTM D 974	<i>Standard Test Method for Acid and Base Number by Color-Indicator Titration</i>
ASTM D 445	<i>Standard Test Method for Kinematic Viscosity of Transparent and Opaque Liquids</i>
ASTM D 5185	<i>Standard Test Method for Determination of additive elements, Wear Metals, and Contaminants in Used Lubricating Oils by Inductively Coupled Plasma Atomic Emission Spectroscopy</i>
ASTM D 1500	<i>Standard Test Method for ASTM Color of Petroleum Products</i>

A newer method for detecting the quality of an oil sample is to measure the electrical properties of the oil to determine the extent of degradation. In this method, a sensor of some type is used to measure the dielectric constant or the change in the dielectric constant of the oil sample. Tests of this method on used oil samples have shown that as an oil sample is degraded, the dielectric constant of the sample will show a marked increase over a similar sample of fresh oil. The underlying principle behind this measurement is not fully understood as of yet but, the leading and most logical theory is that as the oil is degraded, it will take on a stronger dipole characteristic and increase the dielectric constant of the material. <sup>[7-19]</sup>

### 2.1.3 Current Research

There is much current and recent research in the field of sensors for measuring oil quality. Some commercial sensors are even available at a premium price. In this section I will discuss some of the more relevant information that I have used as guidance for my project.

Research published by Turner and Austin has shown a distinct and definite correlation between increased use and thus degradation of an oil sample and an increase in the dielectric constant of used oil samples. In their research, used oil samples of a known mileage were collected and the viscosity and dielectric constant of each sample was taken and plotted against one another. The resultant plot (Figure 2.2) showed that the more the oil was used and the greater the degradation, the higher the measured dielectric constant was.<sup>[7]</sup>

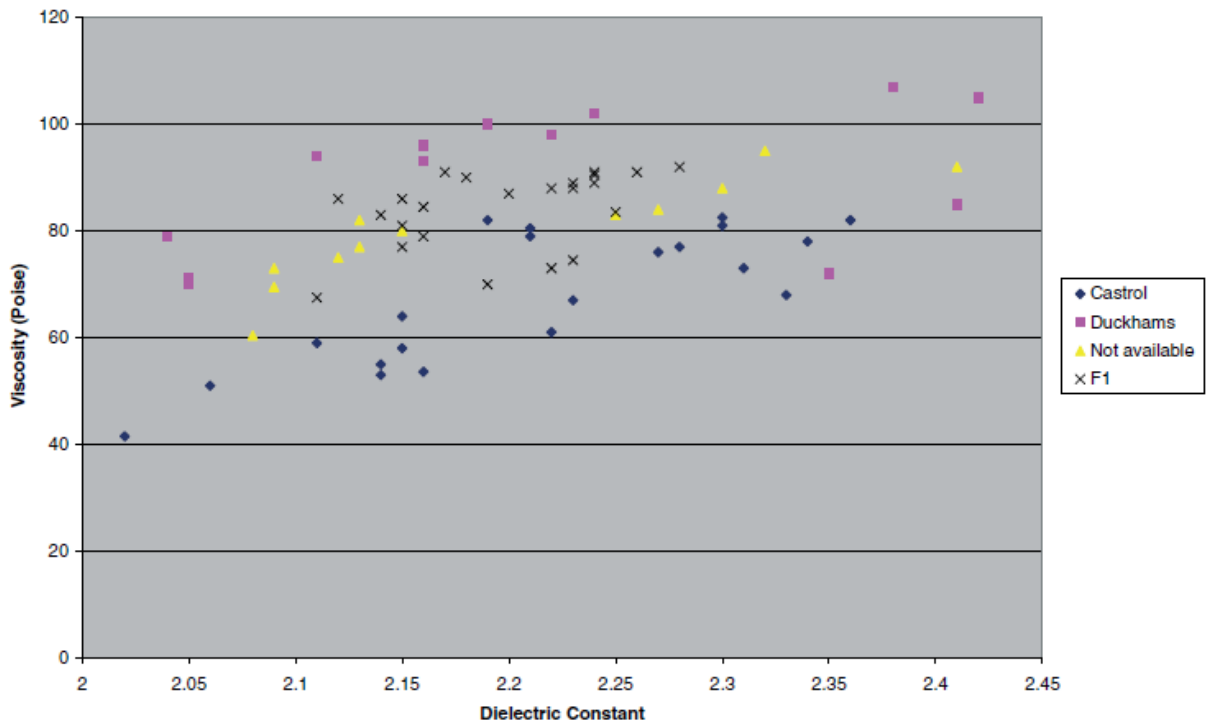


Figure 2.2 Lubricating oil viscosity vs. dielectric constant.<sup>[7]</sup>

Research performed by Lee, Kim and Semenov has shown some other useful information regarding the measurement of the dielectric properties of lubricant oils.<sup>[8]</sup> First, they showed how the dielectric constant of lubricant oil changes with temperature. They measured 14 types of fresh oil at temperatures ranging from room temperature to 100 C. The results, shown in Figure 2.3, show that the dielectric constant change is related to the type of oil and the chemical makeup of it but, at temperatures less than 60 C, the dielectric constant stays in a range between 2.2 and

2.4 depending on manufacturer. This will determine how the sensor can be implemented, if placed in too warm of an environment, the data collected might be misleading.

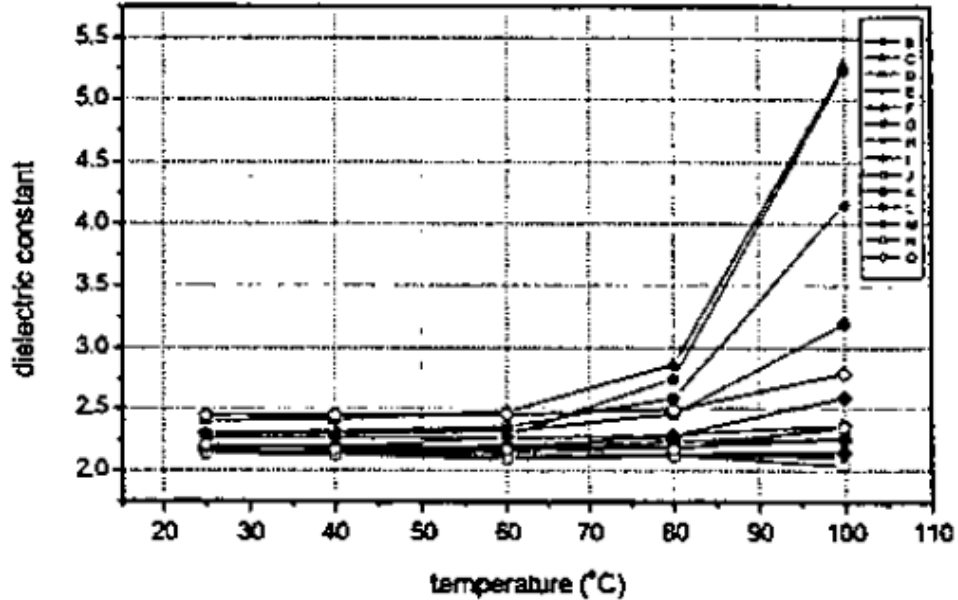


Figure 2.3 Change of dielectric constants with temperature of fresh oil.<sup>[8]</sup>

The three researchers also developed a sensor to detect the deterioration of oil in situ. Their approach was to use a coil capacitive sensor that was inserted into the oil pan. Their sensor uses two enamel coils wound together to measure the cross capacitance of the oil. They compared these measurements to independent measurement of dielectric constant to determine if the sensor was detecting the change. Their results show the sensor capacitance at 11pF in air, 22 pF in the fresh oil and 23.6 pF in oil that had been used for 16,000 km. The tests were done for different oils and different distances travelled. Figure 2.4 shows the plot of the their results, it shows the correlation between the measured capacitance and the independently measured dielectric constant of the oils.<sup>[8]</sup> Overall, their research helps to show the feasibility of using a capacitance sensor to measure the deterioration of engine oil.

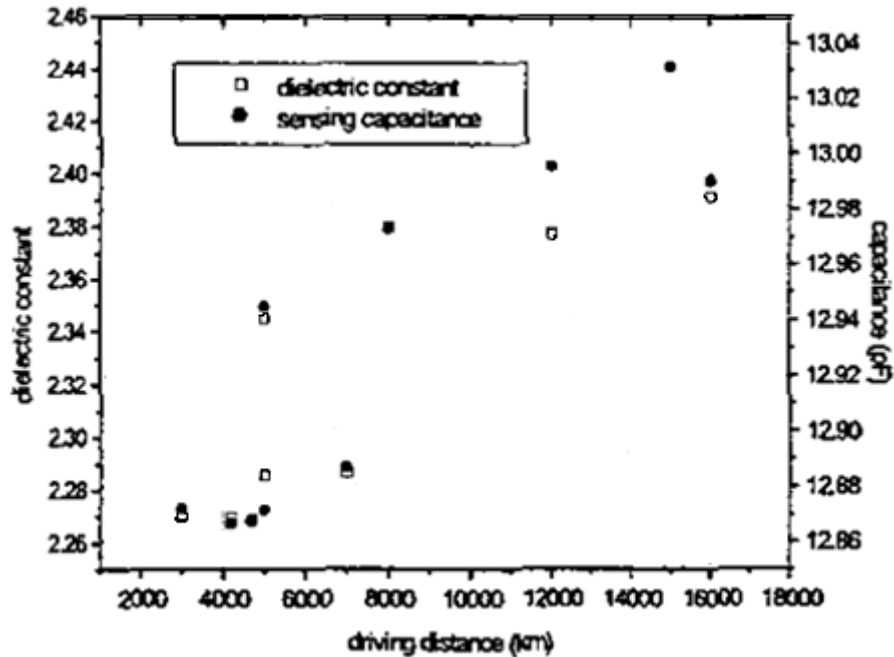


Figure 2.4 Correlation between the measured dielectric constant and the sensing capacitance.<sup>[8]</sup>

Additional researchers have also investigated the coil type capacitive sensor and the relationship between the dielectric constant of oil and its temperature.<sup>[9]</sup> Their data on dielectric constant and temperature correlates with that of Lee, Kim and Semenov shown in Figure 2.5. Up until about 55 or 60 C, the dielectric constant remains relatively stable but it increases above that temperature, varying with the composition of the oil. They continued on by investigating how the dielectric constant changed with use. The oil was run in engines on a dynamometer for up to 20,000 km and then the dielectric constant was measured at various temperatures. This again shows in Figure 2.6 that the dielectric constant will increase with use and also that the temperature that the constant is measured at has an effect on the result.

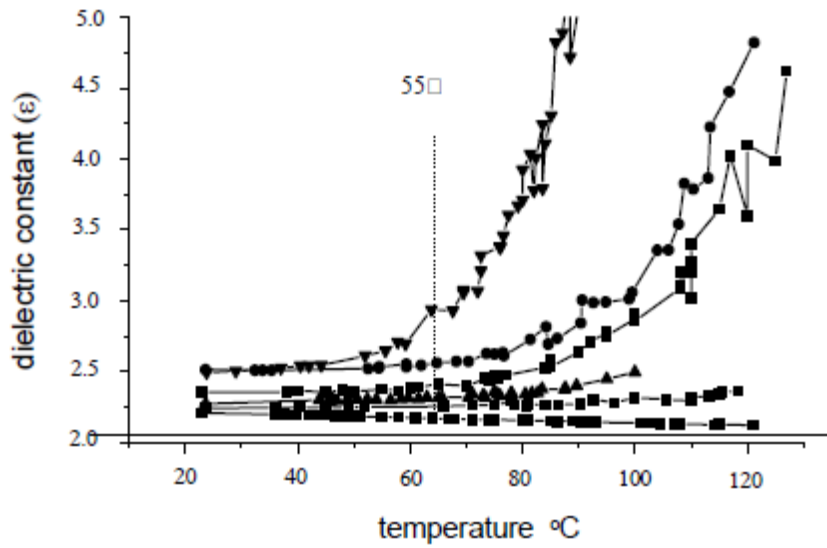


Figure 2.5 Characteristics of dielectric constant vs. temperature for engine oil.<sup>[9]</sup>

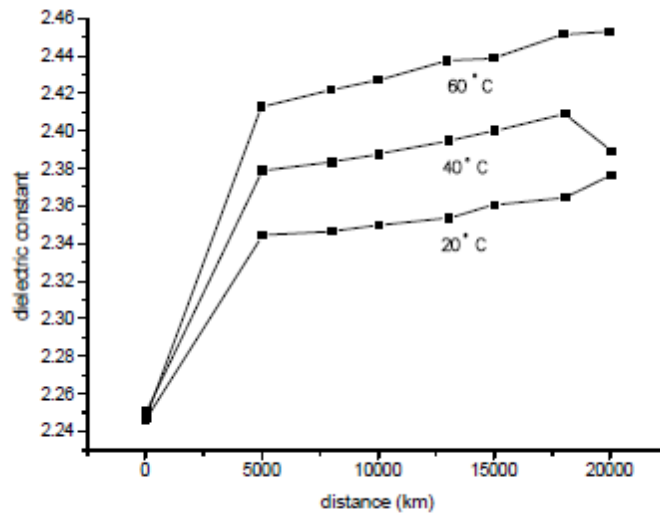


Figure 2.6 Dielectric constant vs. driving distance and its variance with temperature.<sup>[9]</sup>

The work of Raadnui and Kleesuwan<sup>[10]</sup> also shows that the dielectric constant of oil will change as it is used and is degraded. Their experiment used a grid capacitor to measure the change in capacitance and then determine the resulting change in dielectric constant. By taking measurements in air as a control and then in fresh and used engine oil they showed that the

change in the dielectric constant and thus the condition of the oil can be monitored with a capacitance sensor. Figure 2.7 shows their results for measured dielectric constant in air and in fresh and used oil at several frequencies.

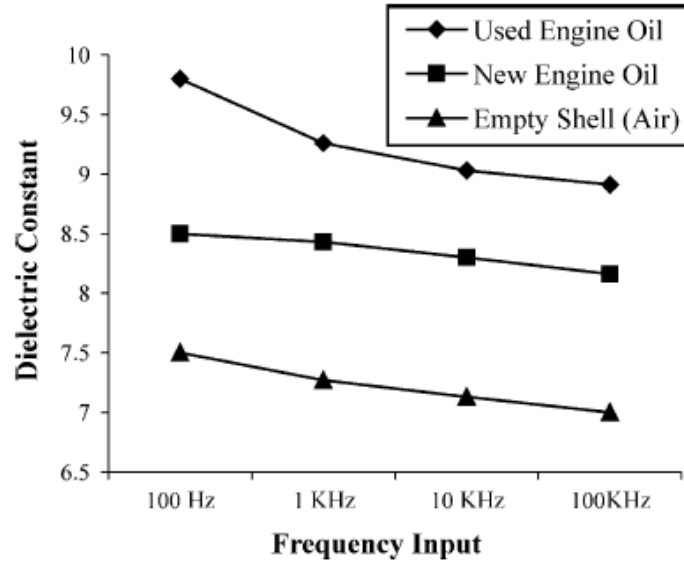


Figure 2.7 Measured Dielectric Constant for grid capacitance sensor in various media.<sup>[10]</sup>

Raadnui and Kleesuwan have also done investigations on the effects of various contaminants in lubricant oils and how they affect the dielectric constant. In the study, ferrous particles, water and silicon dioxide particles were each introduced into oil samples. Each was mixed in three levels of concentration and the dielectric constant of the sample was measured. The investigation showed that each of the three contaminants had an effect on the dielectric constant. In each case, as the concentration of the contaminant rose, the dielectric constant followed in the same way. However, with the addition of water, there was no change between the first and second concentration.

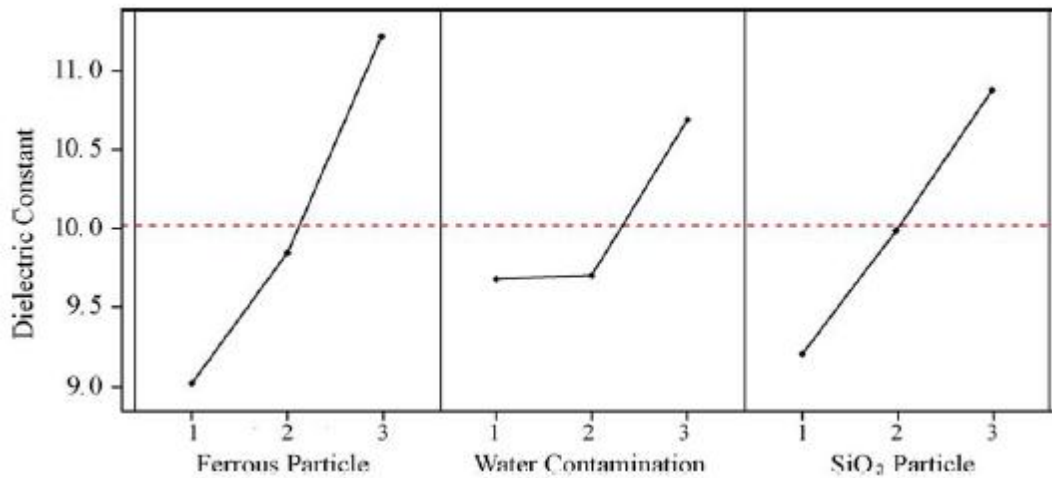


Figure 2.8 Change in the dielectric constant with different concentrations of contaminant particles.<sup>[10]</sup>

Keller and Saba<sup>[11]</sup> also investigated the changes in dielectric constant with degradation of lubricant oil samples. In their tests, they used a dielectric constant meter and also measured the TAN of the samples. Their results again show that the increased degradation leads to an increase in the dielectric constant of the sample. Plots of change in dielectric constant vs. the TAN show that the two are correlated.

Another important aspect shown in their work is that the dielectric constant is not affected only by the degradation of the oil but also the introduction of contaminants that come from natural wear on the moving parts inside of machinery. Their investigation focused on ferro particles suspended in the oil. The results showed a dependence on the particle size, concentration and the amount of time that the sensor was exposed to the oil. With regard to size, bigger particles had the greater effect while the concentration had some, but little effect. The time aspect of the experiment showed that as the particles are allowed to collect onto the sensor, the greater the change in the dielectric constant.<sup>[11]</sup>

Another research group has investigated how dielectric constant and different contaminants are directly related using a capacitance sensor. <sup>[12]</sup> This research lays groundwork for determining that the dielectric constant can be used as an indicator of oil degradation. The researchers tested water contamination, ferrous metal contamination and change in acid number which seem to be the three most important factors in determining the useful remaining life of lubricant oils. The oils that were tested were SF20W/30(A), SF 15W/30(B), SE10W/30(C) and SE5W/30(D). For each of the factors tested, a mostly linear relationship exists between the dielectric constant and an increase in the concentration of the contaminant. Figures 2.9, 2.10 and 2.11 show these relationships graphically for each of the four oil types A-D. Knowing that this correlation exists will allow for further experimentation with capacitive sensors to determine the quality of oil in situ.

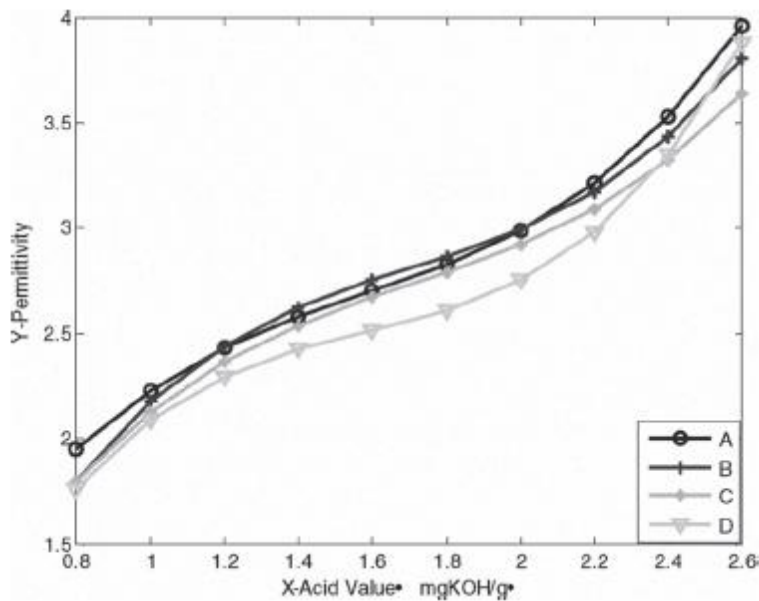


Figure 2.9 Relationship between permittivity (Dielectric Constant) and acid number. <sup>[12]</sup>

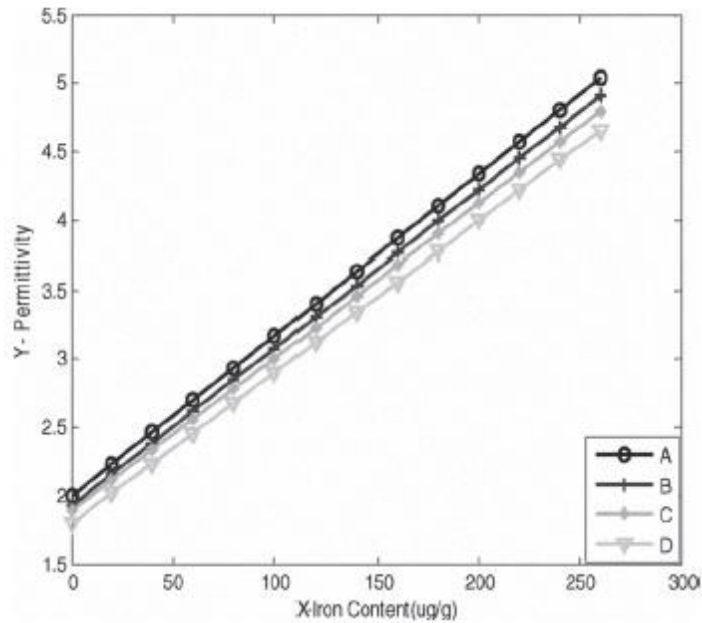


Figure 2.10 Relationship between permittivity (dielectric constant) and iron content. <sup>[12]</sup>

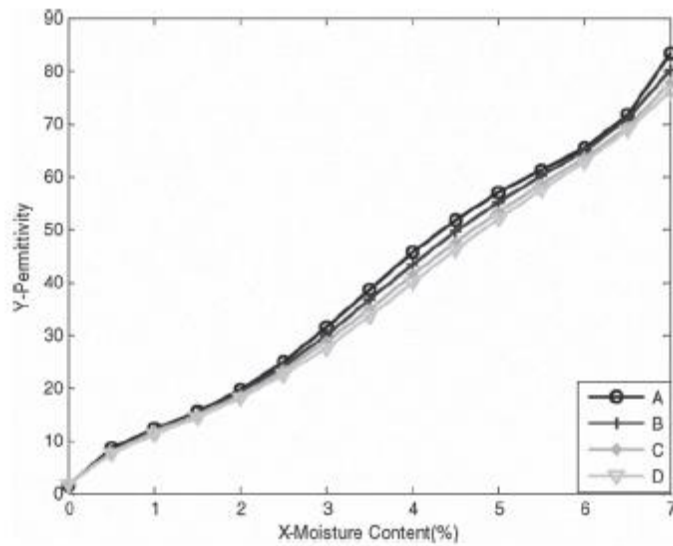


Figure 2.11 Relationship between permittivity (dielectric constant) and moisture content. <sup>[12]</sup>

Yang and his collaborators have also worked at testing the feasibility of using capacitive sensors to detect the change in the dielectric constant of oil. <sup>[13]</sup> Their focus was on how different contaminants affected the dielectric constant measurement. By using a cylindrical capacitive sensor and a series of digital signal manipulations they were able to detect small variances in the

capacitance and thus the dielectric constant of oil samples. They contaminated 4 different oil samples and took measurements, one with water, two with varying amounts of ferrous particles and one with used engine oil. The resulting plot, Figure 2.12, of the relative change in dielectric constant for each contaminant shows that all of these will have an effect on the overall measurement and that the dielectric constant of the oil is a suitable measurement for determining the deterioration of an oil sample. It not only shows chemical changes but also outside pollutants like metal particles and water contamination.

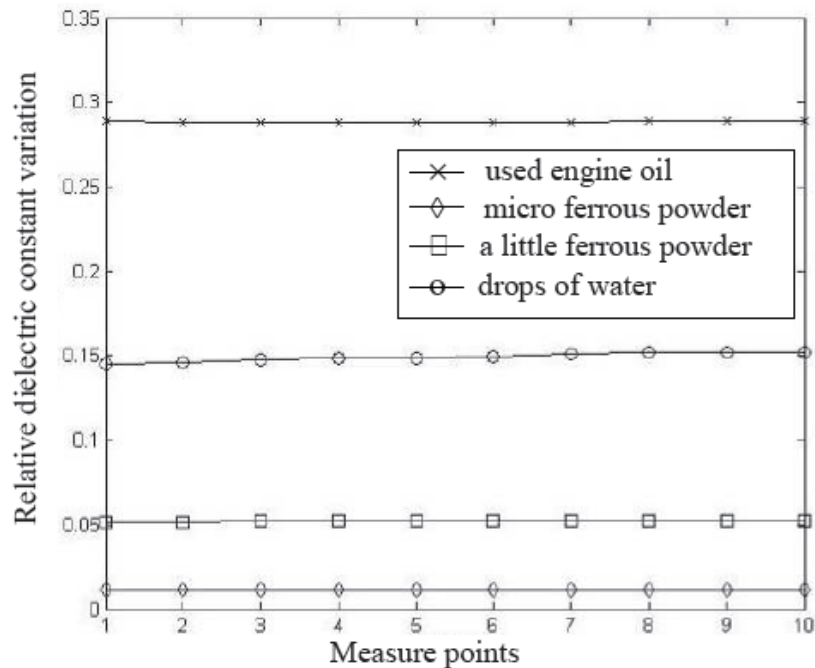


Figure 2.12 Relative dielectric constant variation of different polluted oil samples from fresh oil sample. <sup>[13]</sup>

From all the current research it is clear that a capacitive sensor of some type can be implemented to monitor the condition of lubricant oil in situ. The effects of the oils deterioration chemically and its contamination due to wear and introduction of moisture and other liquid contaminants have been shown to cause increases in the dielectric constant of the oil and thus

related increases in the capacitance. The previous research has used many types of capacitance sensors all based on similar parallel plate concepts. What remains is trying to simplify the design by creating a planar interdigitated electrode to be used as a capacitance sensor and implemented onto a dipstick. The fabrication of such a device would be easier to accomplish and be relatively inexpensive when done on an industrial scale. By taking the research that has already been done and advancing it in this new direction, a new device can be designed and fabricated to achieve similar results in a new form factor using the existing established principles.

#### 2.1.4 Commercially Available Sensor Systems

Several models of vehicles currently in production have what are called oil life monitors. These devices are based on the engine computer measurements. The vehicle's computer collects data on the number of cold starts, the time and distance travelled, the RPMs generated and various other factors. These measurements are then run through an algorithm that can estimate the remaining useful life of the oil. These devices can be useful but a sensor to measure the actual physical condition of the oil, and not an estimate, would be preferable.

One option that is currently commercially available to directly monitor the condition of lubricant automotive and machine oil in situ is from Delphi.<sup>[20]</sup> The Delphi oil quality sensor monitors electrochemical materials that are present in degraded oil. The sensor uses a triangular waveform to make the materials of interest interact with the sensing electrodes and create a current flow. The current flow is measured by the electrode and the oil quality can be determined. Their literature indicates that the magnitude of the current will be proportional to the concentration of the material that is being measured and inversely proportional to the viscosity of the oil. The sensor itself is installed in the oil reservoir and measures in real time. The sensor

measures the TAN, viscosity, water content, temperature and oil level. An illustration of the sensor is given in Figure 2.13.



Figure 2.13 Illustration of Delphi Oil Quality Sensor. <sup>[20]</sup>

## 2.2 Capacitance Sensors

Sensors for the measurement of capacitance values are commonplace in modern devices. The operation is based on a simple formula and can be easily implemented in a variety of situations.

### 2.2.1 General Principles

Capacitance sensors can vary in their type and structure. However most are based on a parallel plate structure that is basic and common. Parallel plate capacitors consist of two plates of a given area set at a distance apart from one another with a dielectric medium of some sort in between the two. The useful part of this relationship is that the capacitance can be calculated by the formula:

$$C = \frac{\epsilon_0 \epsilon_r A}{\delta} \quad (2.1)$$

where  $C$  is the capacitance,  $\epsilon_0$  is the permittivity of free space (a constant),  $A$  is the area of the plates,  $d$  is the spacing of the plates and  $\epsilon_r$  is the dielectric constant of the media between the two plates. By knowing the constant values of  $\epsilon_0$ ,  $A$  and  $d$ , we can determine the dielectric constant of the media that is in between the plates of the capacitor. This also means that the capacitance and the dielectric constant of a material are related. So, as the oil in the experiment ages, the dielectric constant will change and the capacitance of the oil in the sensor will change as well.

### 2.2.2 IDT Structure

For this application, an interdigitated electrode design was chosen. IDTs have been widely used and studied in a variety of capacities.<sup>[21-34]</sup> In this case, it will be used as a capacitive sensor. The IDT design consists of two sets of fingers that interpenetrate making a comb structure. This sets up a series of parallel plate capacitors that can be used as a sensing area. The geometry of the IDT plays a large role in the sensitivity of the structure. The main aspects of the design are the thickness of the fingers, the spacing between the fingers, the width of the electrode and the number of fingers that are used. Each of these factors will affect the measurements that are taken and the sensitivity of the sensor. The sensitivity of the sensor should increase with decreased finger spacing, an increased number of fingers, and increased width and finger thickness.

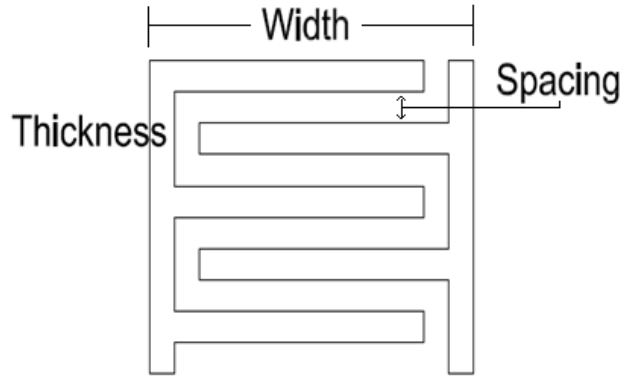


Figure 2.14 Schematic diagram of an interdigitated electrode.

Starting with equation 2.1, it can be seen that by changing the variables that we have control over, namely the area,  $A$ , and the spacing,  $d$ , we can control the expected capacitance measurement of the sensor. In general, increasing the area of the fingers, (this can be done by increasing the thickness, increasing the width and increasing the number of fingers) will increase the capacitance value that the sensor will measure under a given condition. The capacitance measurement can also be increased by decreasing the spacing of the fingers. The increase in the value of the capacitance is beneficial to the sensor because the independent variable, namely the dielectric constant of the surrounding fluid, will multiply that value with its change. This means that as the measured capacitance value increases, the sensitivity to change will also increase. Figure 2.15 illustrates this. In the figure, the capacitance value vs. finger spacing is plotted for constant finger area. The value for the dielectric constant for air used in the calculation is 1 and the value for the dielectric constant for oil used is 2.1. The figure clearly shows an expected trend of increased capacitance values and sensor sensitivity with decreased finger spacing.

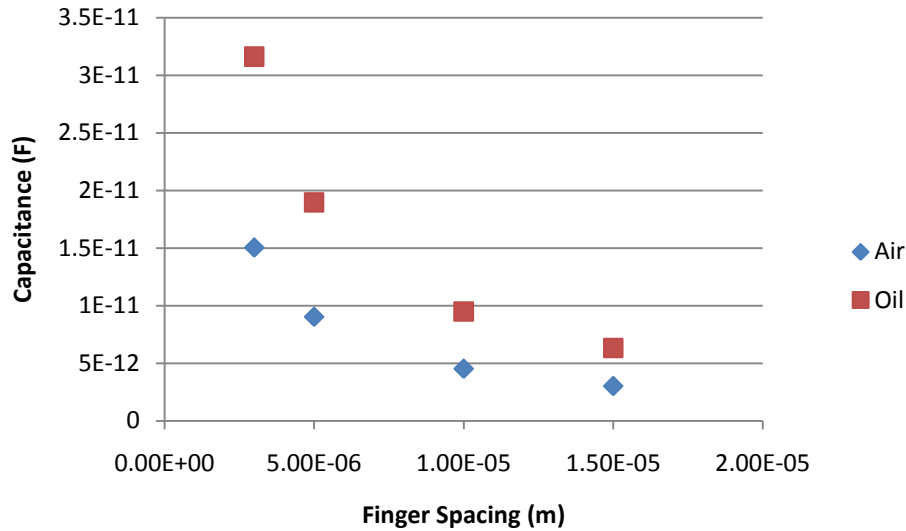


Figure 2.15 Plot of Calculated Capacitance vs. Finger spacing using equation 2.1

### 2.2.3 IDC Model

The modeling of interdigitated capacitors has been the subject of much study. An accurate mathematical model of the IDC would allow for a valuable comparison between the calculated value and the eventual measured value. The model that will be used here was developed by Igreja and Dias and is based on the conformal mapping technique.<sup>[22]</sup> The model is able to take into account a layered structure which gives it an advantage over other IDC models. Figure 2.16 shows the layout of the electrode and the cross section. This model assumes that we can consider the thickness of the substrate as infinite if the thickness is much greater than the spatial wavelength ( $\lambda=2(W+G)$ ). In addition, the thickness of the fingers can be ignored because it is much less than the width. Figure 2.17 shows the equivalent circuit used in the model.



$$C_{E,IDC} = C_{E,media} + C_{E,SiO2} + C_{E,Si}$$

$$= \epsilon_0 L \left( \epsilon_{media} \frac{K(k_{E\infty})}{K(k'_{E\infty})} + (\epsilon_{SiO2} - \epsilon_{media}) \frac{K(k_{E,SiO2})}{K(k'_{E,SiO2})} + \epsilon_{Si} \frac{K(k_{E\infty})}{K(k'_{E\infty})} \right) \quad (2.4)$$

The terms  $k_{I,\infty}$  and  $k_{E,\infty}$  are given by

$$k_{I,\infty} = \sin \frac{\pi}{2} \eta \quad (2.5)$$

and

$$k_{E,\infty} = \frac{2\sqrt{\eta}}{1+\eta} \quad (2.6)$$

The  $k'$  is the complex modulus of  $k$  and is equal to the square root of  $(1-k^2)$ . The variable  $\eta$  is the metallization ratio which is given by  $W/W+G$  which are shown in Figure 2.16. The values for  $k_I$  and  $k_E$  for the finite silicon dioxide layers are much more complex to calculate but take into account the thickness of the layer. A detailed description of how to calculate each is given in Igreja and Dias. In all equations  $\epsilon$  is the dielectric constant of the material and  $\epsilon_0$  is the permittivity of free space. Additionally, Table 2.2 gives the relevant equations for both the finite and infinite conditions.<sup>[22]</sup>

This model can be easily adapted for different structures and add any number of finite layers. It will be used as a point of comparison for the measurements that will be taken with the actual sensors later.

Table 2.2 Equations needed for calculation of CI and CE for finite and infinite layers.<sup>[22]</sup>

	Interior electrodes	Exterior electrodes
Finite layer	$C_I = \varepsilon_0 \varepsilon_r \frac{K(k_I)}{K(k'_I)}$	$C_E = \varepsilon_0 \varepsilon_r \frac{K(k_E)}{K(k'_E)}$
	$k'_I = \sqrt{1 - k_I^2}$	$k'_E = \sqrt{1 - k_E^2}$
	$k_I = t_2 \sqrt{\frac{t_4^2 - 1}{t_4^2 - t_2^2}}$	$k_E = \frac{1}{t_3} \sqrt{\frac{t_4^2 - t_3^2}{t_4^2 - 1}}$
	$t_2 = \operatorname{sn}(K(k)\eta, k)$	$t_3 = \cos h\left(\frac{\pi(1 - \eta)}{8r}\right)$
	$t_4 = \frac{1}{k}$	$t_4 = \cos h\left(\frac{\pi(\eta + 1)}{8r}\right)$
	$k = \left(\frac{v_2(0, q)}{v_3(0, q)}\right)^2$	
	$q = \exp(-4\pi r)$	
Infinite layer	$C_I = \varepsilon_0 \varepsilon_r \frac{K(k_{I\infty})}{K(k'_{I\infty})}$	$C_E = \varepsilon_0 \varepsilon_r \frac{K(k_{E\infty})}{K(k'_{E\infty})}$
	$k_{I\infty} = \sin\left(\frac{\pi}{2}\eta\right)$	$k_{E\infty} = \frac{2\sqrt{\eta}}{1 + \eta}$

## CHAPTER 3

### EXPERIMENTAL SETUP & TECHNIQUES

#### **3.1 Artificial Aging of Oil Samples**

In order to properly test the function of the electrodes, testing must be done on oils that have undergone various amounts of use. This should allow for the observation of how the oil changes with its degradation and what we should look for to tell if the oil is past its useable lubricant level. Instead of placing the lubricants into a functioning engine and allowing them to age naturally, it would be of use to be able to artificially age them in a controlled setting. To do this, the oil is heated beyond its normal use temperature and oxygen is bubbled through it at this elevated temperature. This allows for faster aging times for a greater quantity and for more control over the condition of the oil.<sup>[1-5]</sup>

With this in mind, an oil degradation chamber was constructed to artificially age the oil in a controlled environment. The chamber consists of a stainless steel vessel to contain the oil and a band heater to increase the temperature to a controlled point. Dry oxygen was also introduced into the chamber to allow the oil to oxidize as it would in an engine under normal use. A device to stir and agitate the oil was added to insure that the oil was evenly aged. A valve at the bottom of the container allowed for easy removal of samples without having to shut down the device. Samples of the oil were taken at various time intervals for different aging temperatures usually after 24, 48 and 72 hours. This provides a series of oils at different levels of degradation to test. The oil samples that were used for this experiment were manufactured by British Petroleum

(BP). BP 2380 turbo engine oil was used for test runs. The oil was aged at 200 C for periods of 24, 48 and 72 hours. Data for the fresh oil used is given in Table 3.1. <sup>[35]</sup>

Table 3.1 Data for BP turbo oil 2380

<b>BP Turbo Oil 2380</b>	<b>Test Method</b>	<b>Result</b>
Density @ 15°C, Kg/l	<b>ASTM D1298</b>	<b>0.9749</b>
Kinematic Viscosity, cSt, mm <sup>2</sup> /sec @ 100°C @ 40°C @ -40°C	<b>ASTM D445</b> <b>ASTM D445</b> <b>ASTM D-2532</b>	<b>4.97</b> <b>24.2</b> <b>7950</b>
Total Acid N <sup>o</sup> , mgKOH/g	<b>SAE-ARP5088</b>	<b>0.43</b>
Pour Point, °C	<b>ASTM D97</b>	<b>-57</b>
Flash Point, °C	<b>ASTM D92</b>	<b>265</b>
Evaporative Loss, % (6.5h, 204°C)	<b>ASTM D972</b>	<b>3.0</b>

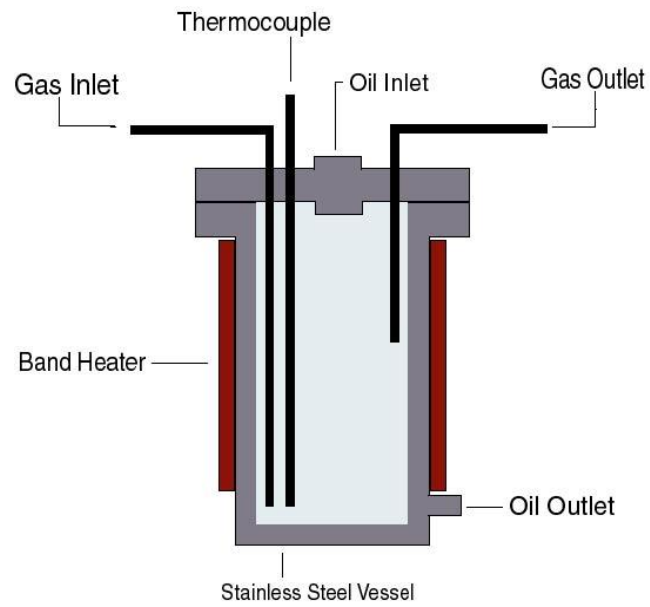


Figure 3.1. Schematic diagram of the oil degradation vessel.



Figure 3.2. Photo of the oil degradation vessel.

### **3.2 Fabrication**

The fabrication of the IDT electrodes used for the experiment was performed using standard photolithography techniques to form the patterns and sputter deposition to deposit the metal electrodes. Photomasks from Covalent Coated Products and Photo Sciences Inc. were used in the lithography process with an nLOF 2035 photoresist. Two substrates were used for the electrodes, SiO<sub>2</sub> and Al<sub>2</sub>O<sub>3</sub>. The SiO<sub>2</sub> for the substrates was thermally grown on silicon wafers and had a nominal thickness of 500 nm. The Al<sub>2</sub>O<sub>3</sub> substrates were deposited via sputter onto silicon wafers and had a nominal thickness of 500 nm as well.

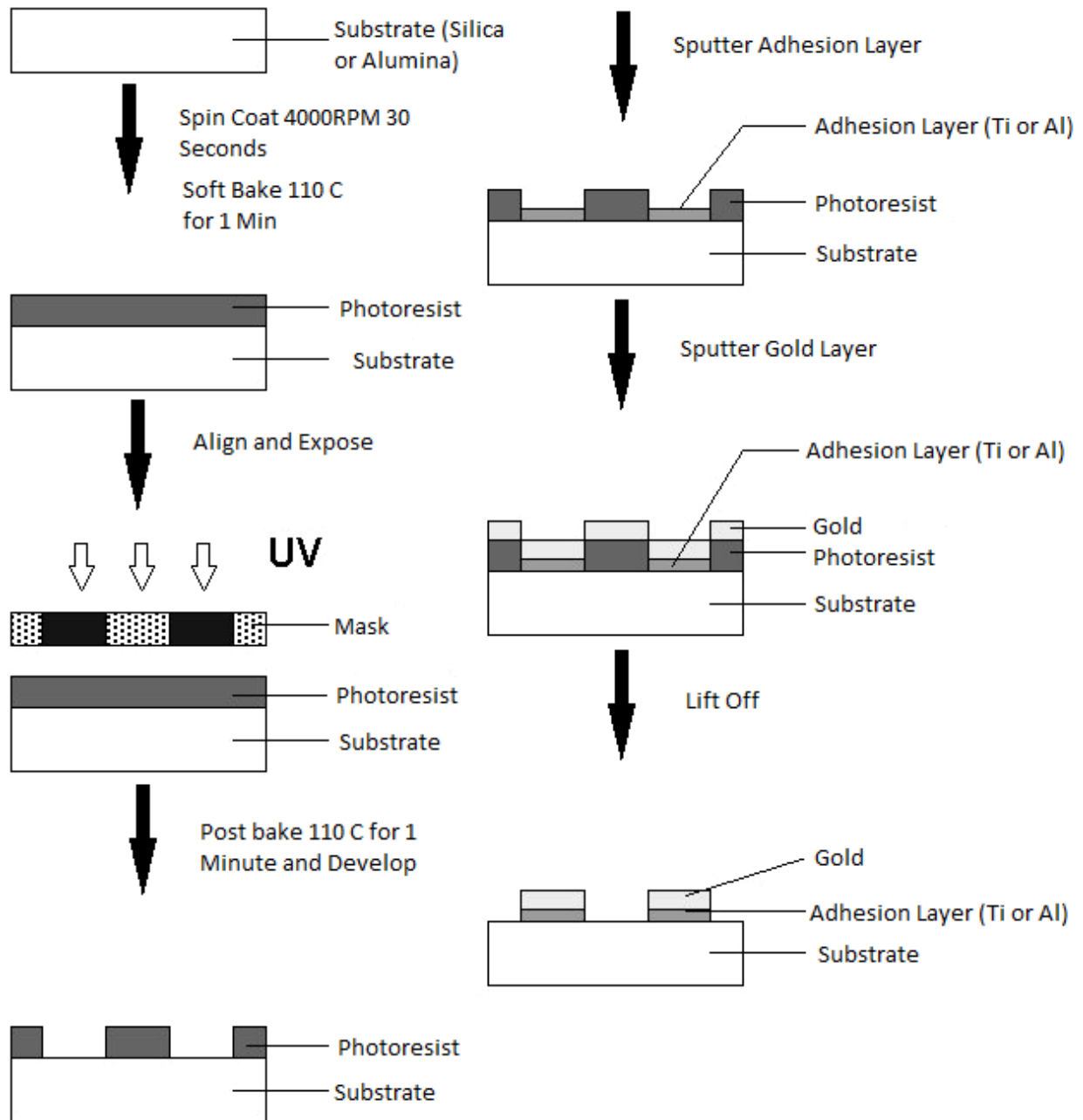


Figure 3.3 Schematic of Fabrication Process. <sup>[36]</sup>

The metallic electrodes were deposited via a DC magnetron sputter system made by Denton Vacuum Inc. The processing is carried out under a high vacuum and high purity argon gas is used as the atmosphere in the chamber. For the SiO<sub>2</sub> substrates, an adhesion layer of either titanium or chromium is deposited first with a thickness of 10 nm. This is followed by the deposition of gold with a thickness of 100 nm. For the Al<sub>2</sub>O<sub>3</sub> substrates, titanium and chromium

did not have the proper adhesion and aluminum was used instead, again with a thickness of 10 nm. In all instances, pre-sputtering was used to clean the target and to stabilize the power to the cathode. All sputter targets are 3 inch diameter. The sputter conditions for the various deposition processes are given in Table 3.2.<sup>[37-43]</sup>

Table 3.2 Sputter Conditions for Metal Depositions.

Material	Pre-Sputter Power (W)	Pre-Sputter Time (Sec)	Sputter Power (W)	Sputter Time (Sec)	Ar Flow Rate (SCCM)	Deposition Pressure (mTorr)	Temp (C)	Ignition Pressure (mTorr)
Gold	<b>100</b>	<b>180</b>	<b>100</b>	<b>180</b>	<b>25</b>	<b>5.0</b>	<b>25</b>	<b>50</b>
Aluminum	<b>200</b>	<b>30</b>	<b>200</b>	<b>30</b>	<b>25</b>	<b>5.0</b>	<b>25</b>	<b>50</b>
Titanium	<b>200</b>	<b>30</b>	<b>200</b>	<b>30</b>	<b>25</b>	<b>5.0</b>	<b>25</b>	<b>50</b>
Chromium	<b>300</b>	<b>30</b>	<b>300</b>	<b>10</b>	<b>25</b>	<b>5.0</b>	<b>25</b>	<b>50</b>

After deposition of the metallic electrodes, the excess metal and photoresist was lifted off in acetone. The wafer was then diced into individual electrodes for testing using a diamond tipped pen to split the silicon wafers.

### 3.3 Measurements

The electrodes that were fabricated for this project are designed to measure the electrical properties of the fluid sample that the electrode is immersed in. In this case, oil is the fluid of interest. For testing, an HP 4192A LF impedance analyzer was used. The instrument can measure a number of variables against a sweep in AC or DC voltage as well as frequency. For this particular experiment, different electrical properties are measured vs. a sweep in the frequency. The electrical properties of major interest are the capacitance, the dielectric loss and the impedance.

The procedure that was used throughout the testing was to first measure the variable that was being tested for the electrode in air. After the air sample was collected, the electrode was

placed in a sample of fresh oil. For this experiment, BP 2380 Turbo engine oil was used. After a fresh oil measurement, the electrode was rinsed in methanol to clean it and then placed in oil that had been artificially aged and another measurement was taken. This was repeated for three different levels of aging and then once more in an oil sample that was aged regularly in a turbo engine.

## CHAPTER 4

### RESULTS & DISCUSSION

The objective for this research is to develop and optimize an IDT sensor electrode to achieve the highest sensitivity to a change in capacitance. The sensitivity of this measurement is important because in future studies it will allow for more accurate determination of the amount of degradation in the oil sample. To reach this goal, it must be determined what factors contribute to the sensitivity and how they can be changed to fit the goals and constraints of this project.

From the study of literature, it has been shown that an interdigitated electrode can be used to successfully measure the capacitance value of a dielectric media. It is also known that the sensitivity of the electrode changes with its design.<sup>[21-34]</sup> The geometry of the electrode will affect its sensitivity so by changing the design parameters of the electrode, an optimum design should be able to be produced.

We can treat the basic interdigitated electrode like a parallel plate capacitor and use the equation for capacitance to predict how it will behave as the design is changed. This will give a starting point for our design and allow for the prediction of expected trends with design change. From the equation, we see that the two variables that can be changed with the design are the area,  $A$  and the spacing of the plates,  $d$ . The spacing will correspond to the spacing between the

fingers in the electrode and the area will correspond to a combination of the electrode's width, finger thickness and number of fingers.

From this, we now have four design parameters that can be easily changed. It is now left to determine what effect each parameter has and how important it will be to the sensitivity of the electrode when tested. To optimize the sensor, each will be tested to determine how it affects the capacitance sensitivity and which are most important to the design. From here, various stages of the testing process are presented.

## 4.1 Capacitance Measurements

### 4.1.1 Effect of IDT Geometry

The original electrode design was a rough starting point to test some of the information gathered from the literature and try and determine some trends in the design. The design parameters are given in Table 4.1. These electrodes are large and have finger spacing's ranging from 40 to 100 microns. Using these electrodes, capacitance vs. frequency curves were generated, see figures 4.1 – 4.4 below. The values that were obtained are very low and may be inaccurate, especially when comparing them to the curves generated by taking the same measurement with the later electrode designs. The measurements for the first set of electrodes are less than a picofarad at most points and the separation between them is even smaller.

Table 4.1 Design parameters for Original IDT electrodes

<b>Sample Identification</b>	<b>Space between electrode (<math>\mu\text{m}</math>)</b>	<b>Width (<math>\mu\text{m}</math>)</b>	<b>Length (mm)</b>	<b># of fingers (Total)</b>
<b>40S</b>	40	40	5	30 (60)
<b>60S</b>	60	60	7.5	30 (60)
<b>80S</b>	80	80	10	30 (60)
<b>100S</b>	100	100	12.5	30 (60)

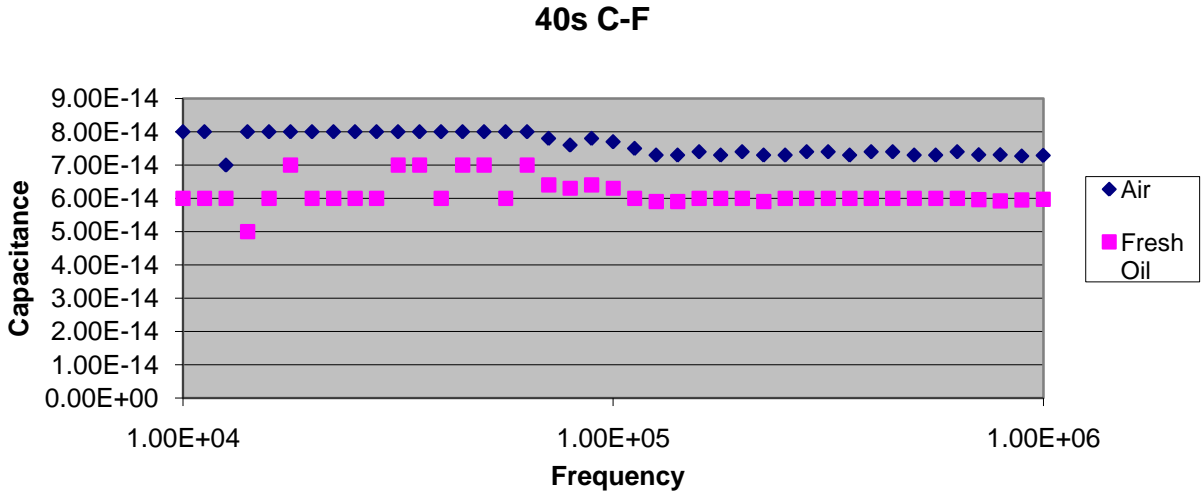


Figure 4.1 Capacitance vs. Frequency curve for 40s electrode.

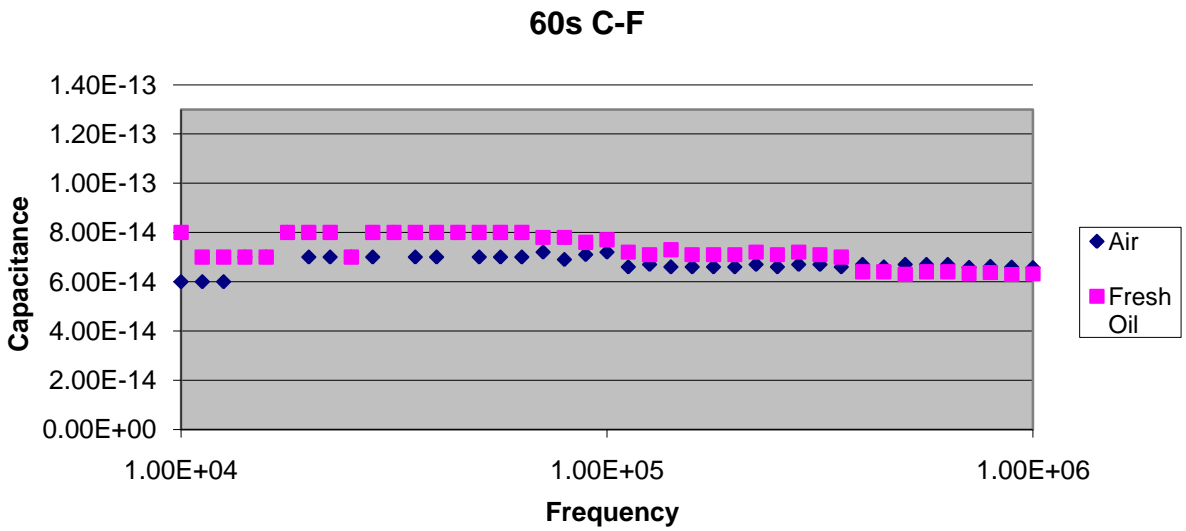


Figure 4.2 Capacitance vs. Frequency curve for 60s electrode.

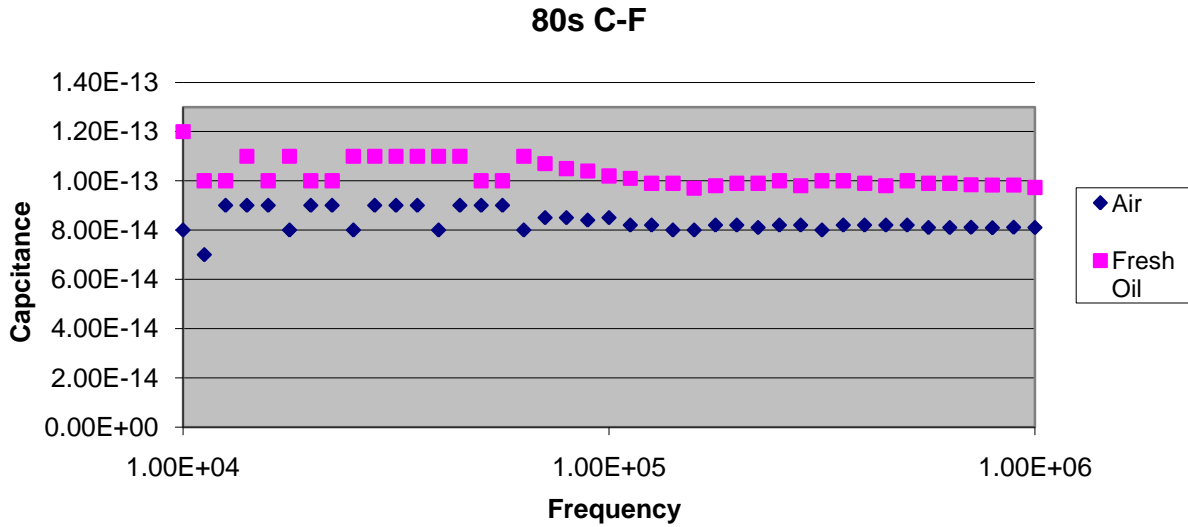


Figure 4.3 Capacitance vs. Frequency curve for 80s electrode.

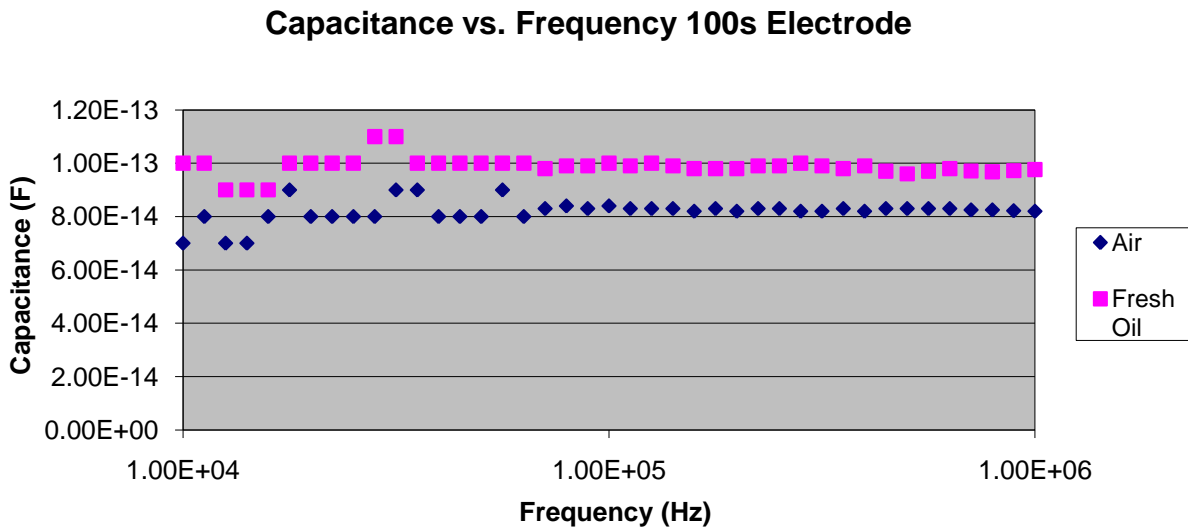


Figure 4.4 Capacitance vs. Frequency curve for 100s electrode.

After the initial testing with the original electrode design, a new design was planned. For this design, it was decided to create the electrodes and vary the four test parameters to determine how changing them would affect the sensitivity and if the trend generated by the sensors would match the expected trend. The design table, Table 4.2, shows the four parameters that are considered. It was decided to vary the thickness of the fingers, the spacing of the fingers, the

number of fingers and the width of the electrode. By testing these parameters it could be determined how each affects the sensitivity of the sensor.

Table 4.2 Design parameters for the second set of IDT electrodes.

<b>Finger Thickness(um)</b>	<b>Finger Spacing (um)</b>	<b>IDT Width (mm)</b>	<b>Number of Fingers</b>	<b>ID</b>
40	100	4.25	60	T4S10F6
40	80	4.25	60	T4S8F6
40	60	4.25	60	T4S6F6
40	40	4.25	60	T4S4F6
40	20	4.25	60	T4S2F6
40	80	8.5	60	T4S8F6L
40	60	8.5	60	T4S6F6L
40	40	8.5	60	T4S4F6L
40	80	4.25	30	T4S8F3
40	60	4.25	30	T4S6F3
40	40	4.25	30	T4S4F3
40	80	4.25	90	T4S8F9
40	60	4.25	90	T4S6F9
40	40	4.25	90	T4S4F9
80	80	4.25	60	T8S8F6
80	60	4.25	60	T8S6F6
80	40	4.25	60	T8S4F6

The following section shows some capacitance vs. frequency curves for these electrodes. In general, they all show the same basic trend. The figures show the series of IDTs with a constant finger width of 40 microns and a spacing of 60 microns. The variation is first, in the number of fingers and then in the length of the fingers. With increasing number of fingers, the capacitance that is measured becomes greater as it also does with the increase in the length.

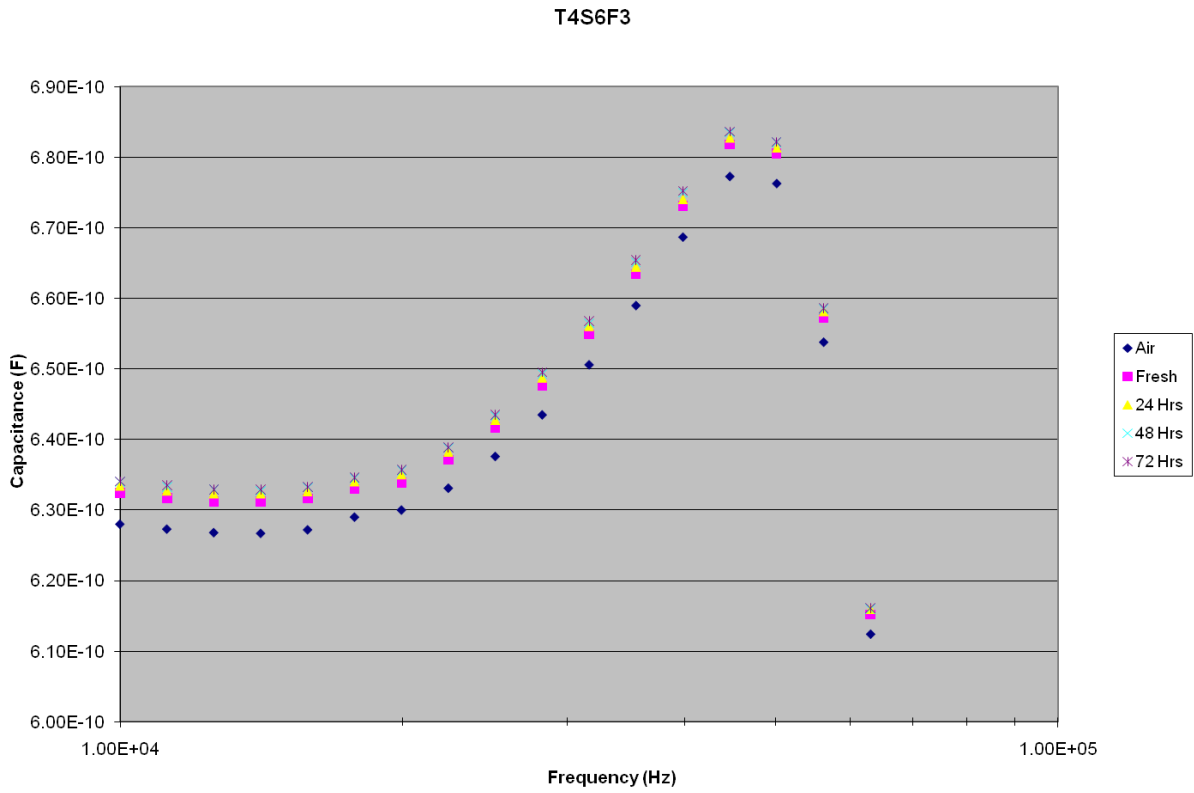


Figure 4.5 Capacitance vs. Frequency curve for T4S6F3 electrode.

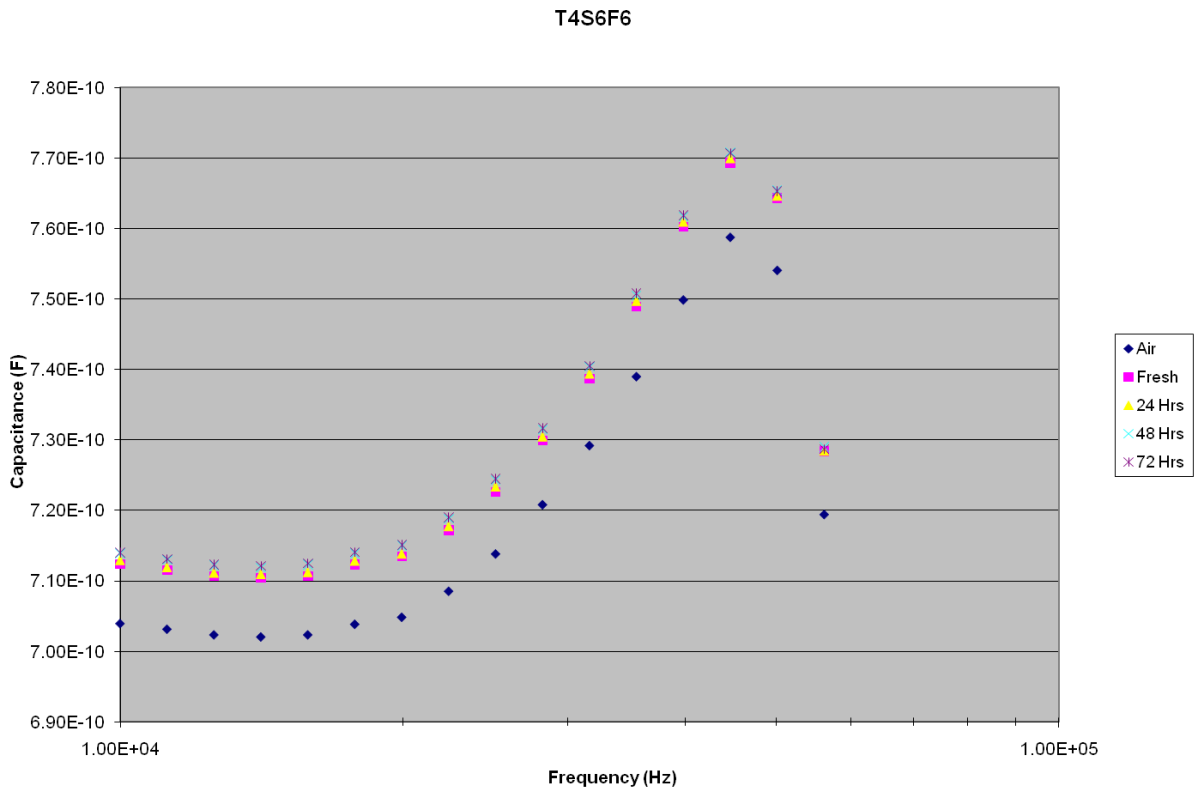


Figure 4.6 Capacitance vs. Frequency curve for T4S6F6 electrode.

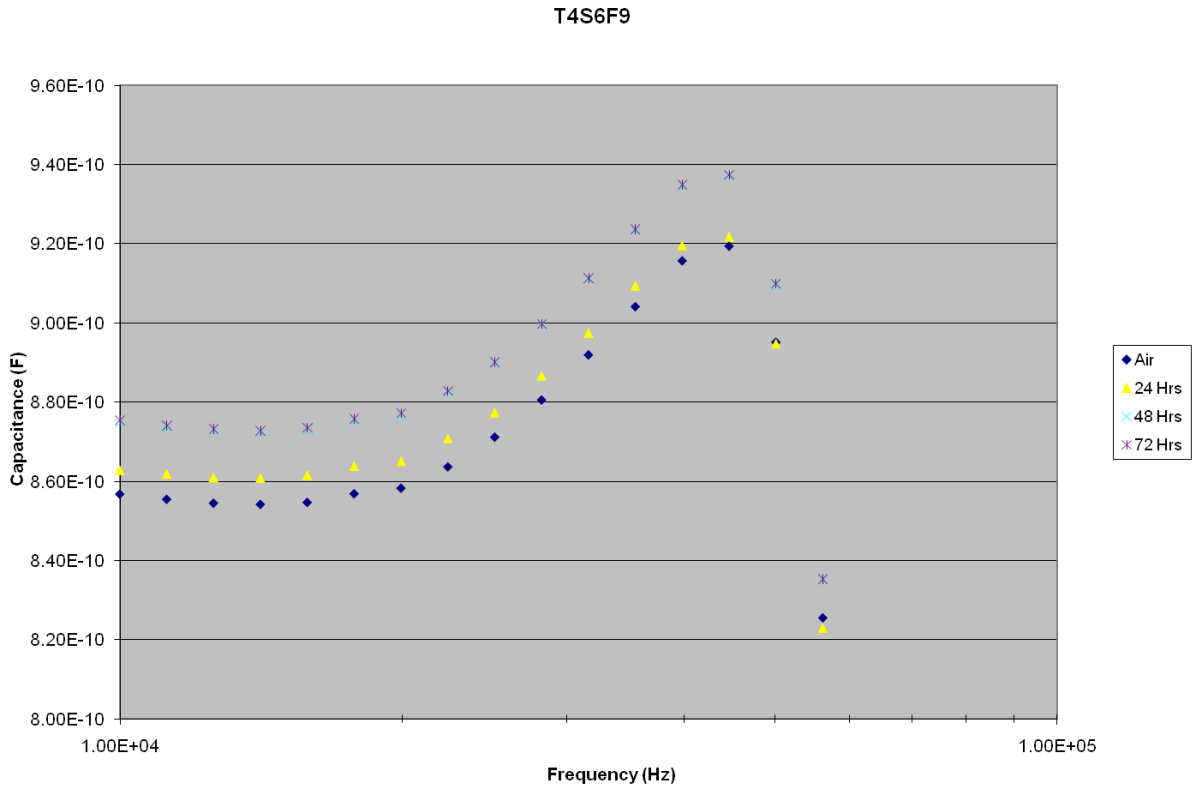


Figure 4.7 Capacitance vs. Frequency curve for T4S6F9 electrode.

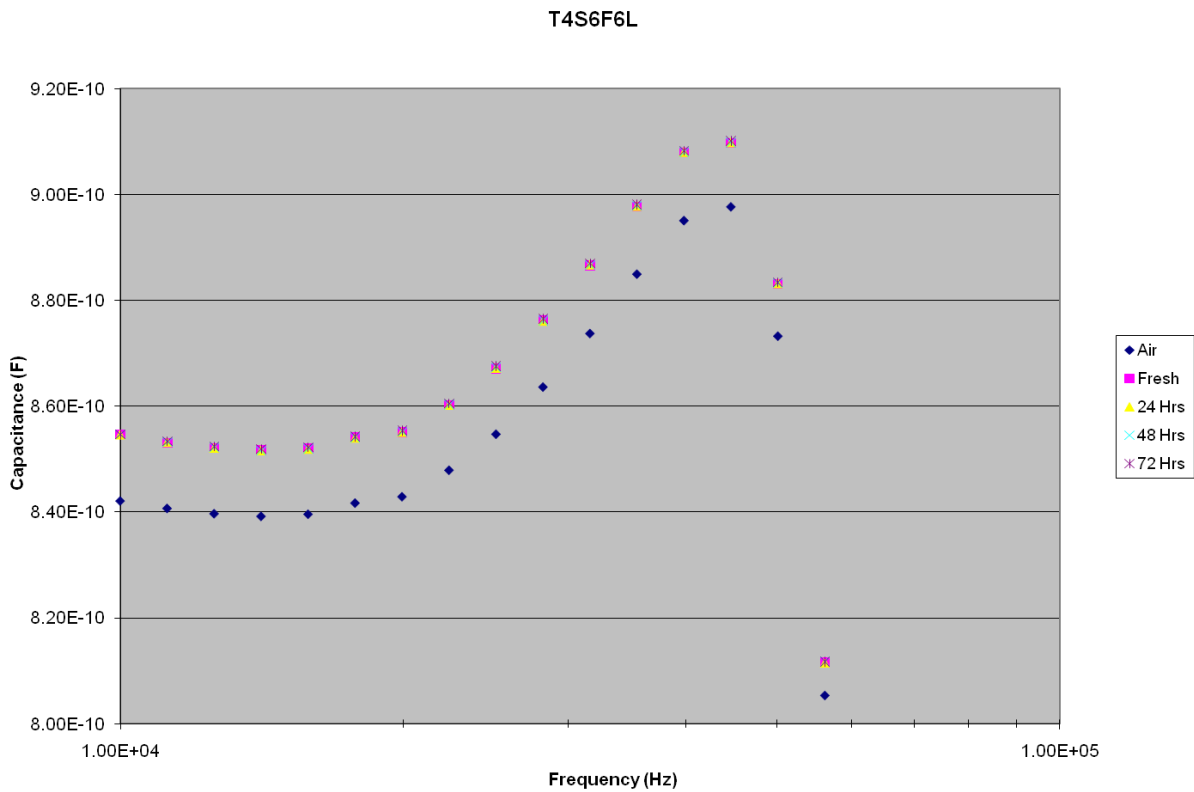


Figure 4.8 Capacitance vs. Frequency curve for T4S6F6L electrode.

From this and the other similar series, it can be shown that some relevant trends are present in the data. By taking the difference between the capacitance value measured in air and the capacitance value measured in fresh oil, the parameter delta C can be used to determine the sensitivity of the sensors and what kind of trend the sensors follow. First, the trend with finger spacing can be shown in Figure 4.9 to have a strong relationship with the sensitivity, as expected. As the finger spacing decreases, the amount of change in the capacitance increases.

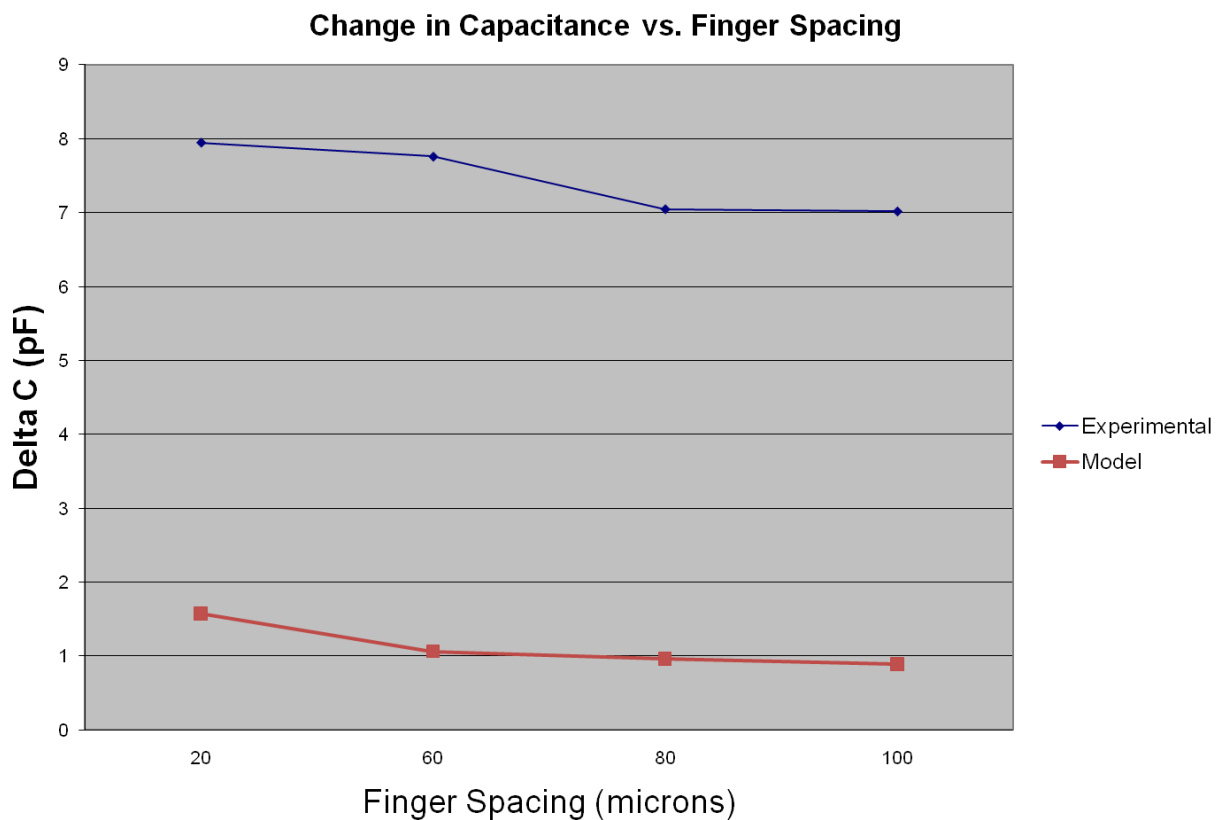


Figure 4.9 Change in capacitance vs. finger spacing.

Figures 4.10 and 4.11 show the trends with change in number of fingers and change in electrode width respectively. Figure 4.10 shows that the sensitivity is maximum at a 60 finger electrode design. This does not agree with what is expected from the literature and the model. The sensitivity should be increased with the number of fingers due to an increase in the overall

area of the electrode that comes with additional fingers. Figure 4.11 shows the increase in sensitivity with increase in electrode width as expected.

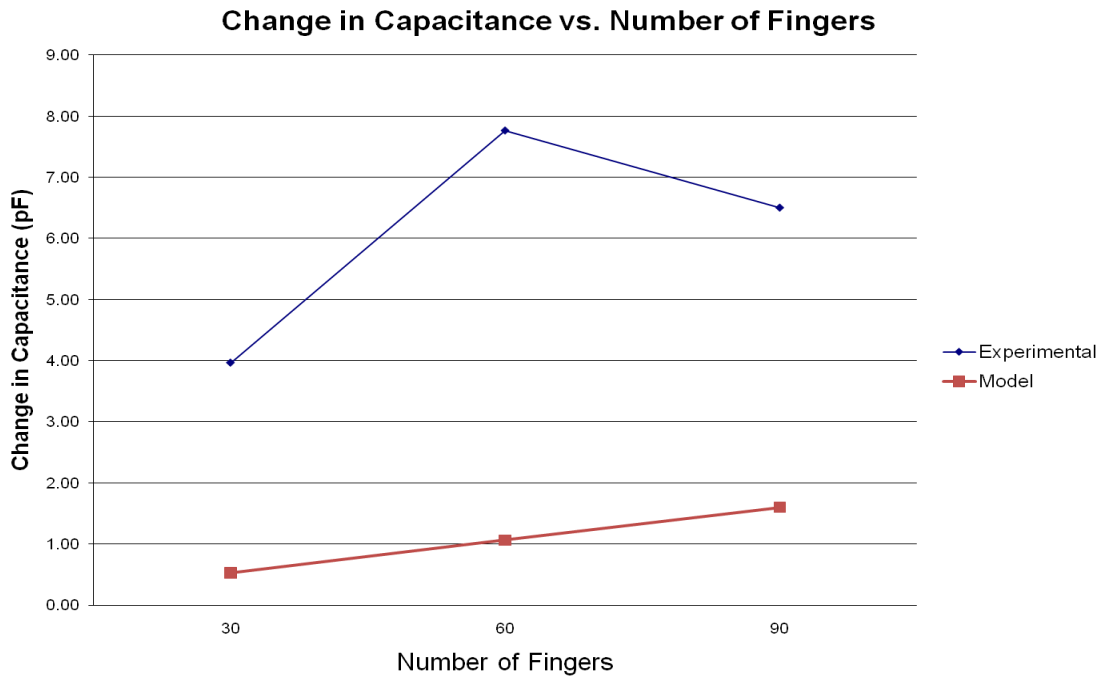


Figure 4.10 Plot of number of fingers vs. the change in capacitance.

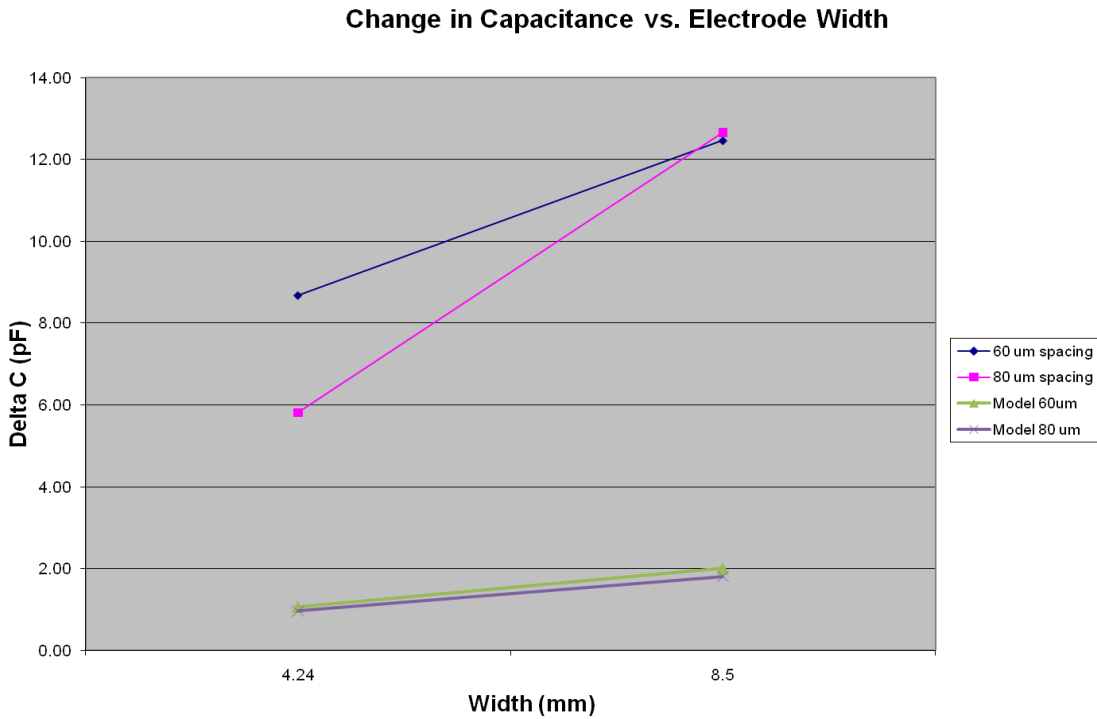


Figure 4.11 Plot of change in capacitance vs. the electrode width.

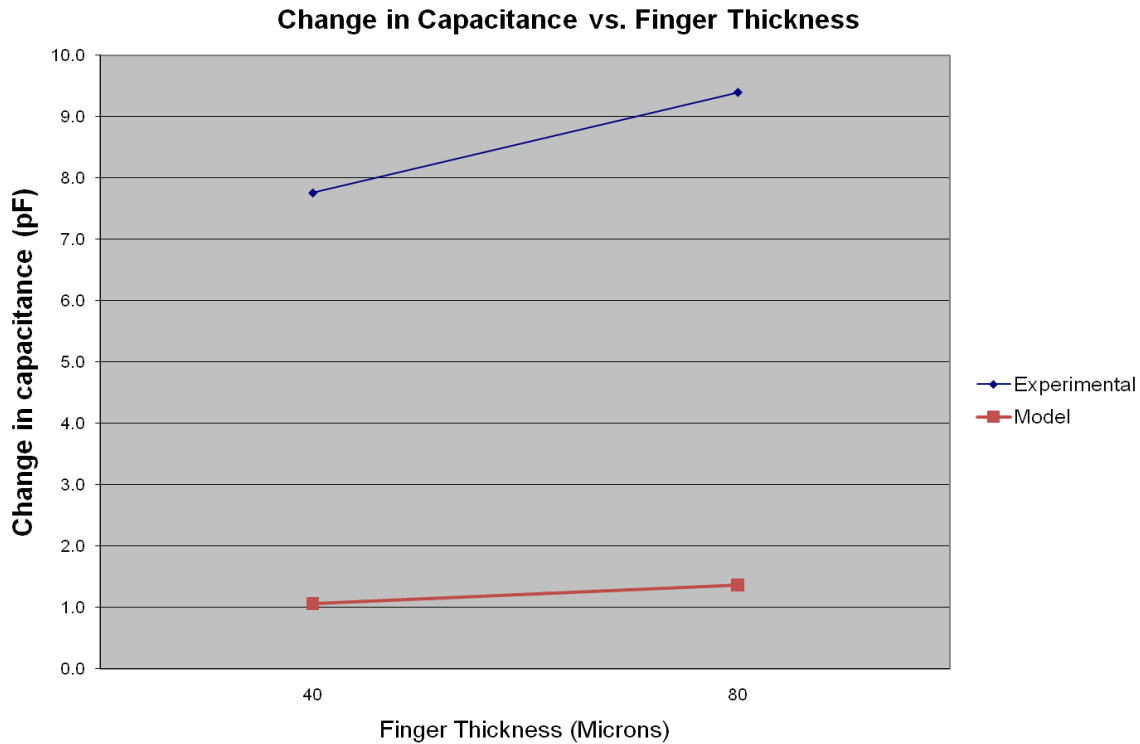


Figure 4.12 Finger thickness vs. Change in capacitance.

Figure 4.12 also shows a useful trend in the data. It shows that as the thickness of the fingers is increased, the sensitivity is increased as well. This is again as expected; the increase in the thickness of the fingers will yield a greater area in the capacitor and thus a greater capacitance measurement and more sensitivity for detection.

In Figures 4.9 through 4.12, the values gained from studying the model are shown in addition to the measured values that were discussed. In all cases, the measured change is greater than that predicted by the model. The possible causes and factors that may contribute to this will be discussed in more detail later. Important to note is that the model and measured values do show the same trends in all but the case for number of fingers.

After analyzing the trends that were observed by testing this series of electrodes, a third and final series was designed and fabricated. The dimensions of these electrodes are given in

Table 4.3. For this set, the finger spacings were minimized to try and achieve maximum sensitivity, with sizes ranging from 15 microns to as small as 3 microns.

Table 4.3 Design parameters for the final IDT electrode design.

<b>Finger Thickness(um)</b>	<b>Finger Spacing (um)</b>	<b>IDT Width (mm)</b>	<b>Number of Fingers</b>	<b>ID</b>
20	15	4.25	60	T2S15F6
20	10	4.25	60	T2S10F6
20	5	4.25	60	T2S5F6
20	3	4.25	60	T2S3F6
20	10	8.5	60	T2S10F6L
40	15	4.25	60	T4S15F6
40	10	4.25	60	T4S10F6
40	5	4.25	60	T4S5F6
40	3	4.25	60	T4S3F6
40	10	8.5	60	T4S10F6L

From the previous data and the information collected in the literature review, it should be clear that the design of the new sensors should provide an increased resolution and ability to detect the changes in the capacitance of the oil samples. The same types of tests were run with the new sensors as for the previous sets. Capacitance vs. Frequency curves for these are shown in Figures 4.13-4.17. Also included in the plots are the values predicted by the model. A large discrepancy between the measured and calculated value is seen in all cases. To determine the problem, different methods of attaching the sensors to the impedance analyzer were tried first. This yielded the same results as previous. Next, a new impedance analyzer was used, and again the same measurements were gathered leading me to believe that the measurements are accurate and that something must be causing the discrepancy between the measurements and the model.

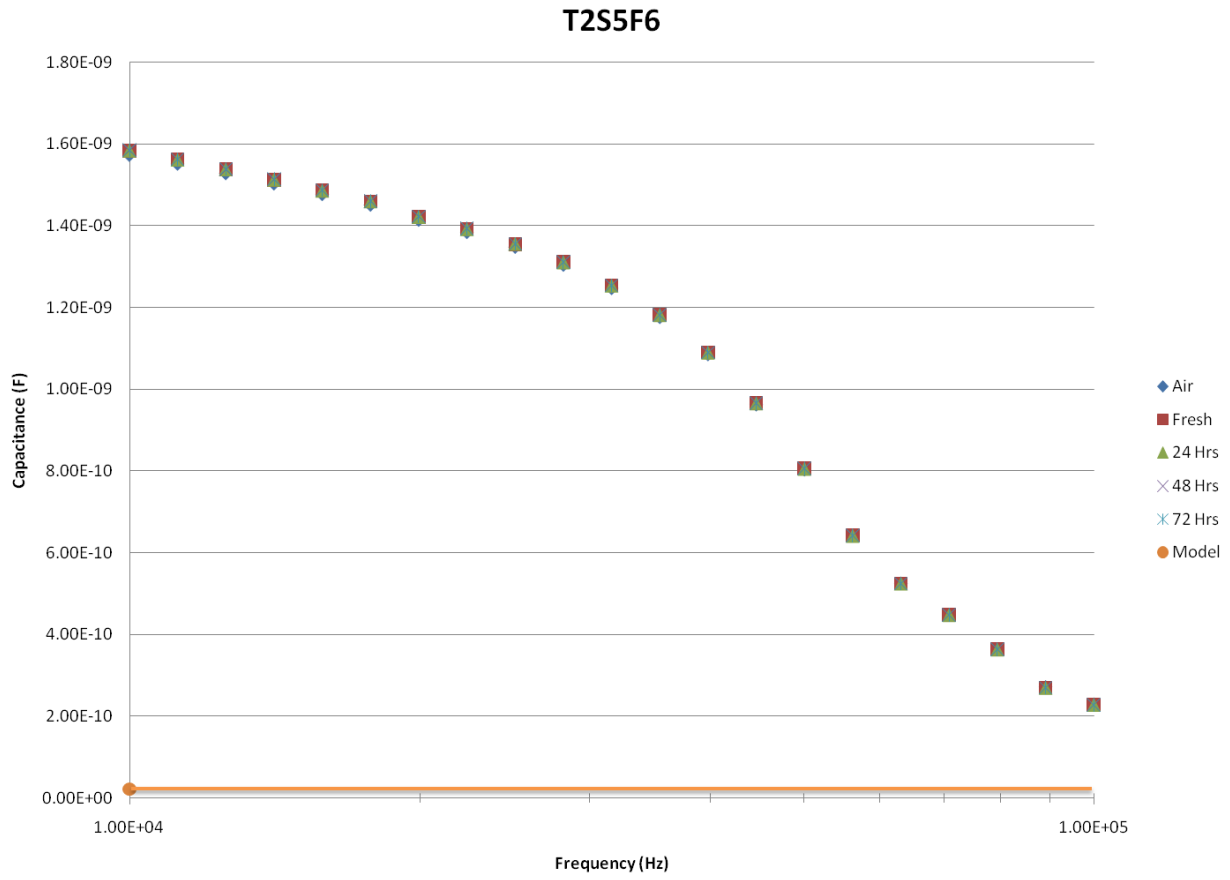


Figure 4.13 Capacitance vs. Frequency curve for T2S5F6 Electrode.

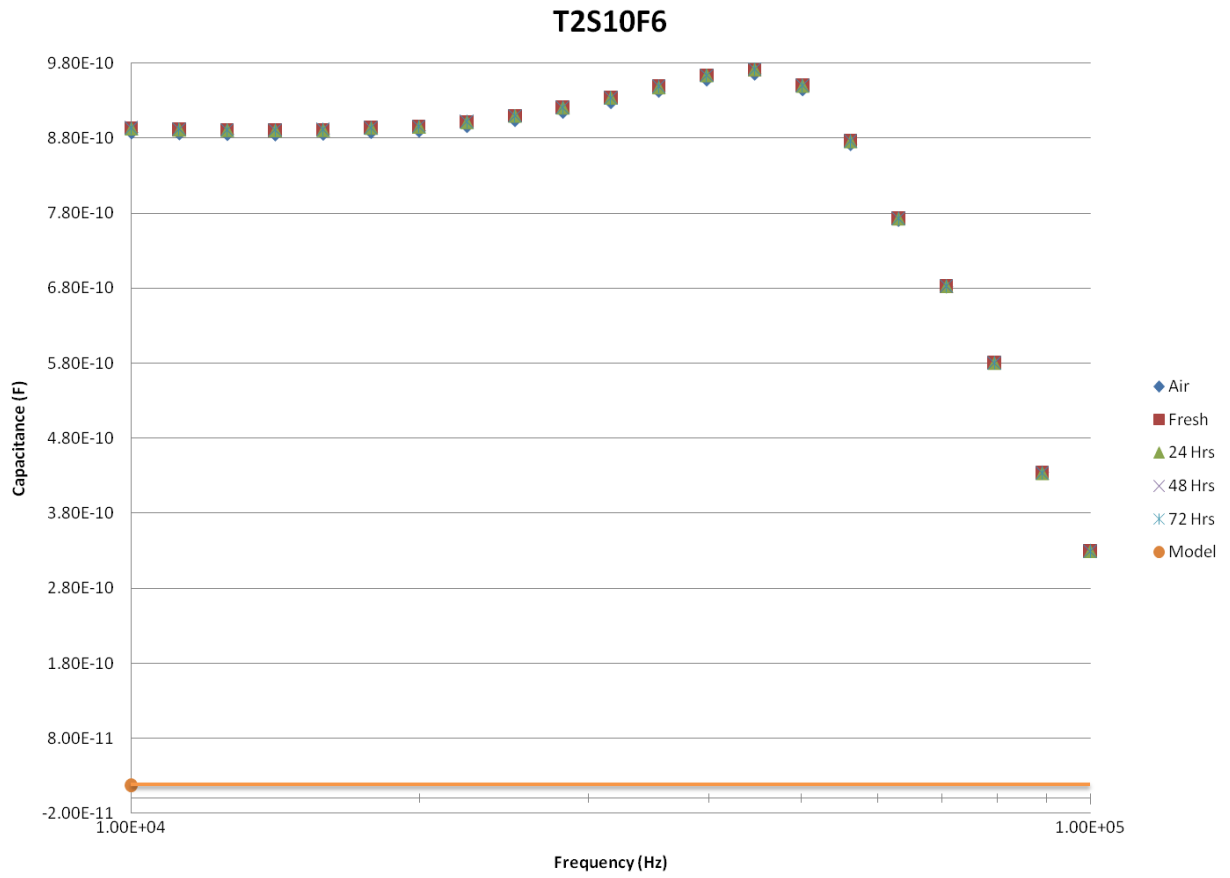


Figure 4.14 Frequency vs. Capacitance curve for T2S10F6 Electrode.

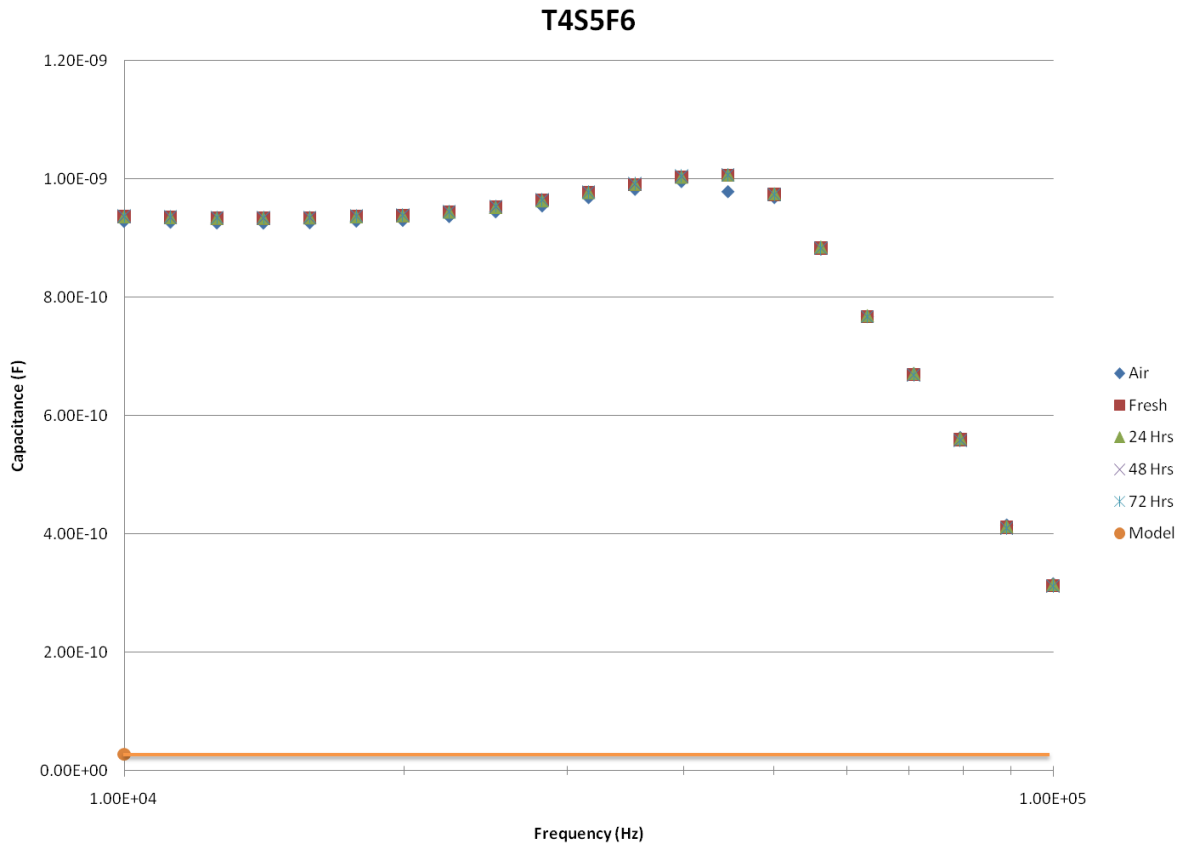


Figure 4.15 Capacitance vs. Frequency curve for T4S5F6 electrode.

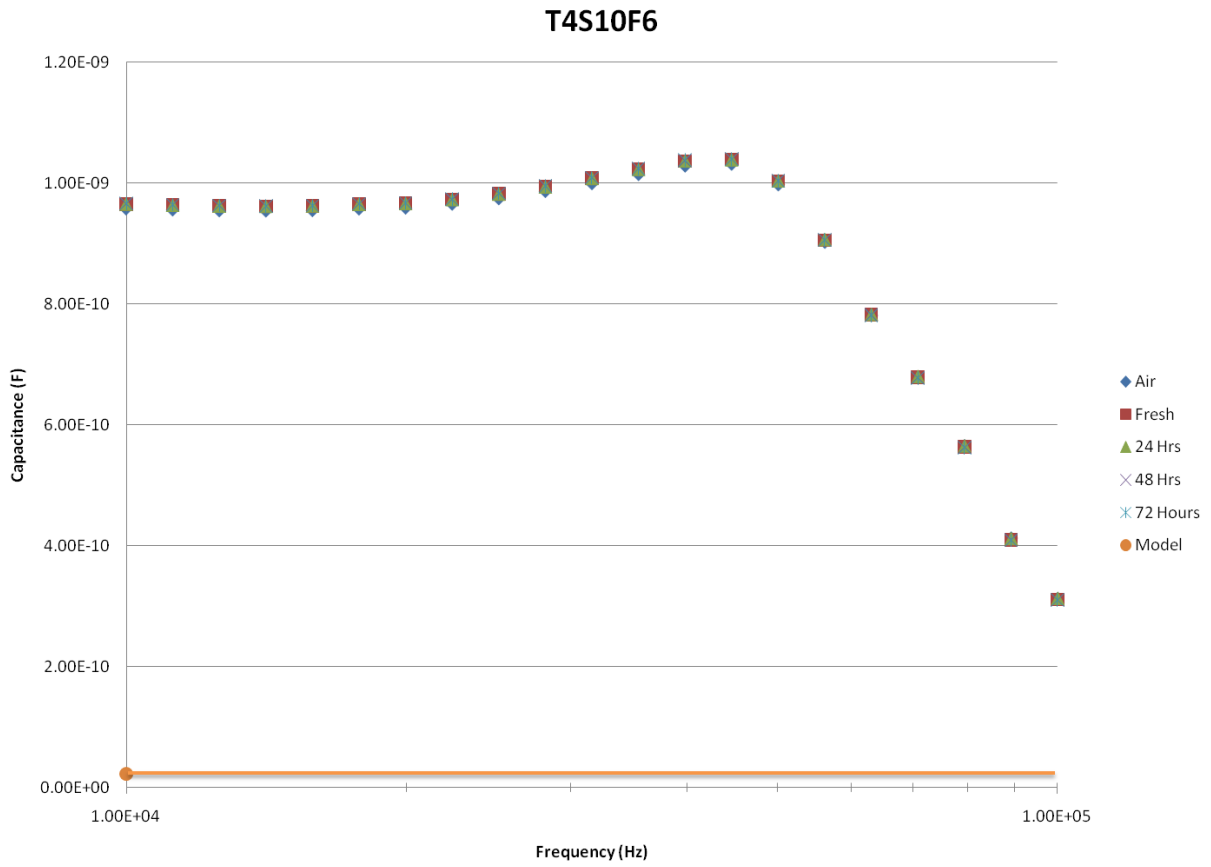


Figure 4.16 Capacitance vs. Frequency curve for T4S10F6 electrode.

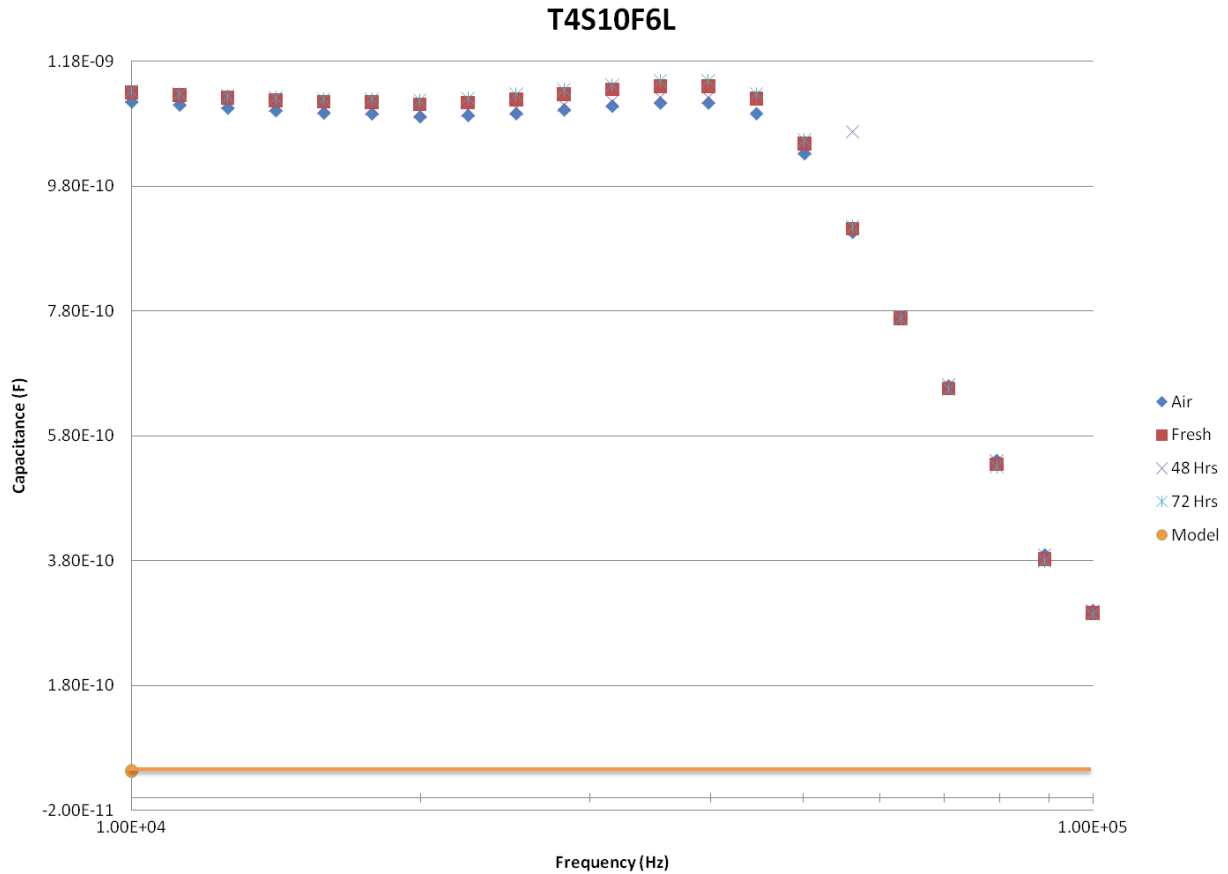


Figure 4.17 Capacitance vs. Frequency curve for T4S10F6L electrode.

The gap between the measured values and the calculated values from the model are much too large to be ignored. As previously discussed, the measurements have been taken with a variety of methods and using separate impedance analyzers so it seems that the equipment is not a major cause of the problem.

The first possible cause that was investigated was to recalculate the model values without assuming that the silicon layer was infinite. Originally the capacitance values were calculated using this assumption and it was thought that changing to a finite layer would both better show a correct prediction of the value and decrease the gap between the measured and modeled values. For this, the model equation 2.3 was modified and became

$$\begin{aligned}
C_{I,IDC} &= C_{I,media} + C_{I,SiO_2} + C_{I,Si} \\
&= \varepsilon_0 L \left( \varepsilon_{media} \frac{K(k_{I\infty})}{K(k'_{I\infty})} + (\varepsilon_{SiO_2} - \varepsilon_{media}) \frac{K(k_{I,SiO_2})}{K(k'_{I,SiO_2})} + \varepsilon_{Si} \frac{K(k_{I,Si})}{K(k'_{I,Si})} \right) \quad (4.1)
\end{aligned}$$

and the value for  $k_{I,Si}$  and  $k'_{I,Si}$  were calculated using the equations from Table 2.2. The new model takes into account the finite thickness and no longer assumes an infinite substrate as before.<sup>[22]</sup>

The result was that there was an increase in the value of the model capacitance but the increase was quite small, at around 5%. This could be a factor but is most likely not the main thing affecting the measurements. Related to this is the actual dielectric constant of the silicon being used. In the model, the assumption was that bare silicon with a silicon dioxide layer was used. However, the wafers used were actually doped. This change could lead to an increased dielectric constant in the silicon and a higher value for the model as well.

Another possible factor that was explored was that the adhesion layer might be causing an increase in the measured capacitance values. The adhesion layer that is present between the silicon dioxide and the gold metallization layer may have oxidized and be causing an increase in the measured capacitance value that is not considered in the original model. To take this into account, Equation 4.1 was further modified to include the additional layer. The new equation is given as

$$\begin{aligned}
C_{I,IDC} &= C_{I,media} + C_{Adhesion\ Layer} + C_{I,SiO_2} + C_{I,Si} \\
&= \varepsilon_0 L \left( \varepsilon_{media} \frac{K(k_{I\infty})}{K(k'_{I\infty})} + (\varepsilon_{Adhesion\ Layer} - \varepsilon_{media}) \frac{K(k_{I,AdLayer})}{K(k'_{I,AdLayer})} + (\varepsilon_{SiO_2} - \right. \\
&\quad \left. \varepsilon_{media} \frac{K(k_{I,SiO_2})}{K(k'_{I,SiO_2})} + \varepsilon_{Si} \frac{K(k_{I,Si})}{K(k'_{I,Si})} \right) \quad (4.2)
\end{aligned}$$

which now takes the addition of the adhesion layer into account.<sup>[22]</sup> The dielectric constants of titanium and chromium oxides are very high and could easily cause a large increase in the measured capacitance if they are present. When the model was adjusted to include an oxidized adhesion layer, the capacitance values of the model increased by up to 5 times the original value. This large increase due to a very thin layer leads me to believe that this is the major cause of the gap between the calculated values of the model and the actual measured values.

Figure 4.18 Below shows a comparison of the different models to each other and the expected value. There is still quite a large gap, but the oxidation of the adhesion layer and taking into consideration that the silicon layer is finite explains what should be causing a large part of the gap.

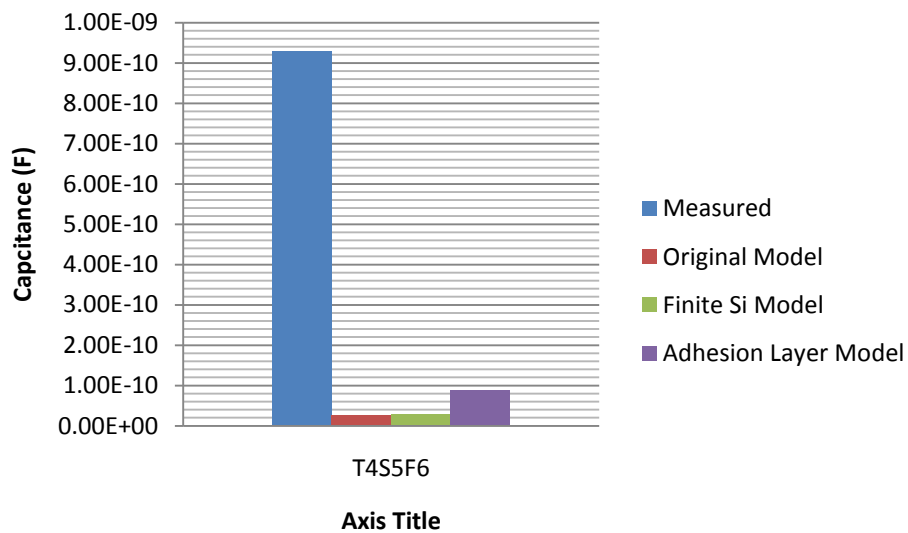


Figure 4.18. Comparison between measured value and the various models used.

The trends in the data for the final electrode design again show what is expected, that a decrease in the spacing between the electrode fingers and an increase in the electrode’s sensing area are preferable. Plots of the change in capacitance vs. the various parameters are shown in Figures 4.19 – 4.21.

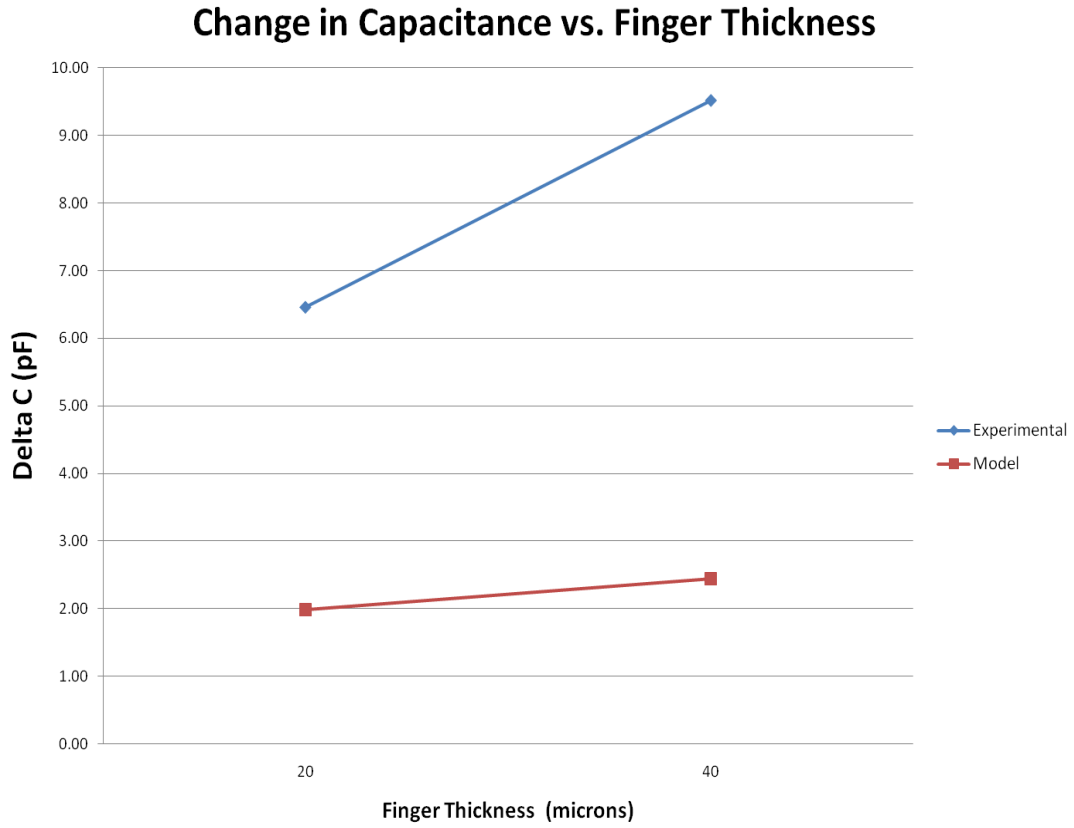


Figure 4.19 Change in capacitance vs. Finger Width.

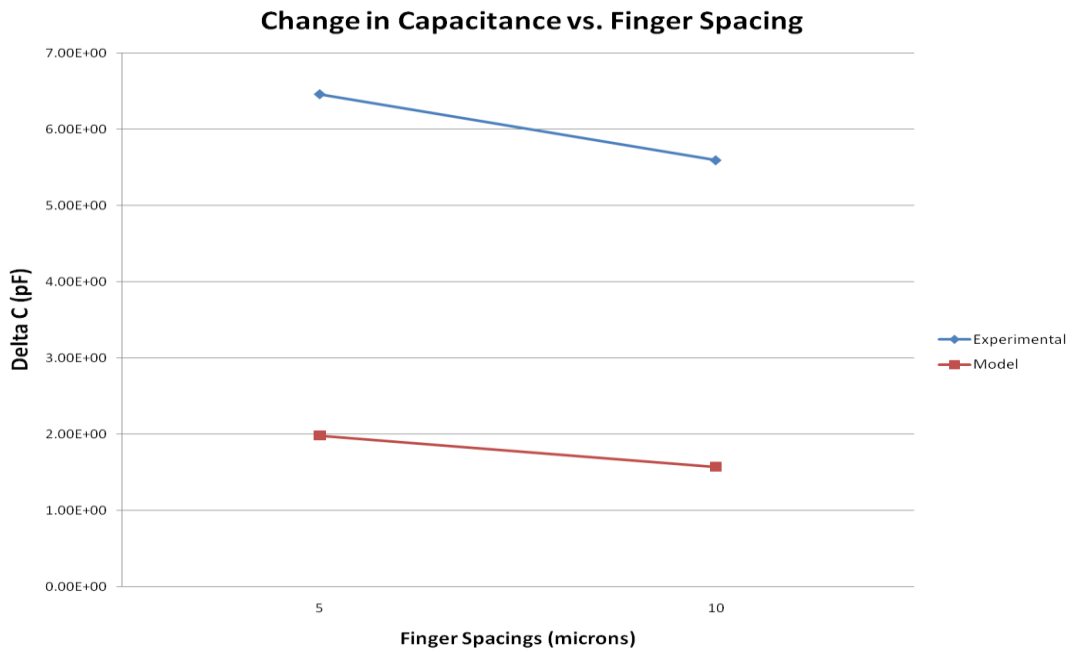


Figure 4.20 Change in capacitance vs. Finger spacing.

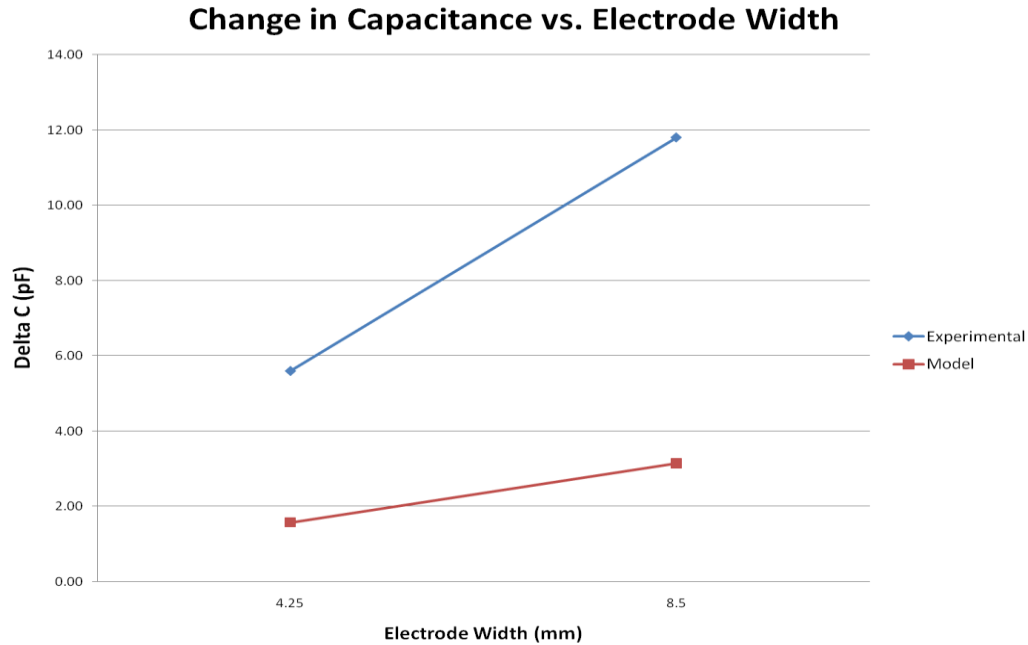


Figure 4.21 Change in Capacitance vs. Electrode Width.

From observing the trends in the data it is clear that by increasing the sensing area and decreasing the spacing between the electrode fingers, the greatest resolution will be possible. This is also shown in the data that is shown in Figures 4.19-4.21. In these plots, the difference is again seen between the modeled values and the measured values like before. This should again be caused mainly by the adhesion layer oxidation and the assumption of the substrate layer to be infinite. The T4S10F6L electrode performed the best when comparing oil to fresh air. It had a difference of 11.8 pF between the two. However, it would be beneficial to determine how much influence each parameter has on the sensitivity measurement and how best to design the electrodes to increase sensitivity. Table 4.4 shows a summary of how each of the factors affects the measurement.

Table 4.4. Effect of design factors on capacitance measurements.

<i>Parameter</i>	<i>Parameter</i>	<i>Delta C</i>	<i>Parameter</i>	<i>Delta C</i>	<i>% Change</i>	<i>Expected %</i>
	<i>Value 1 (μm)</i>	<i>1 (pF)</i>	<i>Value 2 (μm)</i>	<i>(pF)</i>		<i>Change</i>
Finger Spacing	10	5.59	5	6.46	15.5%	26.1%
Finger Thickness	20	6.46	40	9.51	47.3%	23.3%
Electrode Width	4,250	5.59	8,500	11.8	111%	100%

First, if the finger spacing is considered, in both sets of electrodes a strong trend is shown toward an increased resolution with decreased spacing, which is to be expected. It can also be seen that the change in sensitivity that is caused by changing the spacing depends very much on size. For example, the change from a 100 micron gap to a 20 micron gap results in only a about a 13% change in resolution while the change from 10 microns to 5 microns results in almost a 19% increase in resolution. As the spacing becomes smaller, a small change has a much greater effect on the resolution.

Next, if the finger thickness is considered, the trend that is shown is that an increase in the thickness will result in improved resolution, which again is what was expected. For this parameter, the effect seems to not be influenced as much by the absolute size of the electrode. For example, when the thickness of the fingers is doubled from 20 microns to 40 microns, the increase in sensitivity is about 45% and when the thickness is increased from 40 microns to 80 microns the sensitivity increase is about 25%. So, there is still dependence on size but not as much as with the finger spacing.

Finger spacing and finger thickness each have a measureable effect on the capacitance but are not independent of one another. They are more correctly described by the metallization ratio,  $\eta$ . The metallization ratio is equivalent to the thickness divided by the combined value of the thickness and the spacing. It is a measurement of the amount of area covered by the electrode. The capacitance value will increase with an increase in the metallization ratio.

The next parameter to consider is the sensor width. By increasing the width of the sensor, the area is increased and the sensitivity will go up. This has been shown in both the literature and in the experimental process. The effect of the electrode width has a very strong influence on the sensitivity. From the experimental data, at every electrode size, when the width was doubled from 4.25 mm to 8.50 mm the sensitivity value increased by at least 111%. This seems to be the most effective way to greatly increase sensitivity in the easiest way.

The final parameter, the number of fingers, is also important to consider. It should be that the sensitivity increases with the number of fingers due to the increased area of the electrode. However, it shows that there is a maximum in sensitivity at 60 fingers which is unexpected although the raw capacitance measurements do continue to increase with number of fingers as is expected. This maximum in the sensitivity value lets us know that when designing an electrode that we can increase the value to a maximum number of 60 fingers.

Looking at the data, it seems that the value for the 2<sup>nd</sup> and 3<sup>rd</sup> set of electrodes are about the same, but upon further comparison there is an improvement in performance per unit area between the two sets. Tables 4.5 and 4.6 show the change in capacitance per unit area for each of the sets.

Table 4.5. Capacitance per unit area for the 2<sup>nd</sup> electrode series.

<b>Electrode ID</b>	<b>Delta C (pF)</b>	<b>Sensor Area (mm<sup>2</sup>)</b>	<b>ΔC/Unit Area (pF/mm<sup>2</sup>)</b>
<b>T4S2F6</b>	7.95	15.3	0.52
<b>T4S6F6</b>	7.76	25.5	0.30
<b>T8S6F6</b>	9.40	35.7	0.26
<b>T4S6F6L</b>	12.46	51.0	0.24

Table 4.6. Capacitance per unit area for the 3<sup>rd</sup> electrode series.

<b>Electrode ID</b>	<b>Delta C (pF)</b>	<b>Sensor Area (mm<sup>2</sup>)</b>	<b>ΔC/Unit Area (pF/mm<sup>2</sup>)</b>
<b>T2S5F6</b>	6.46	6.38	1.01
<b>T4S5F6</b>	9.51	11.48	0.83
<b>T2S10F6</b>	5.59	7.65	0.73
<b>T2S10F6L</b>	11.81	15.30	0.77

By taking into account the change in capacitance compared to the size and area of the sensor, the final set of electrodes has a higher change in capacitance per unit area. It shows that with better design, a smaller electrode can be as effective at detecting the change in capacitance as a larger electrode. It also allows for determining how small of a sensor that we may be able to make and still be able to detect a given threshold in capacitance change.

#### 4.1.2 Effect of Substrate Material

So far, all of the models that have been used have not taken into account that the electric field applied to the sensor not only penetrates into the oil or air, but also into the substrate when the tests are being run. To make an effort to determine how the substrate material effects the measurements and the sensitivity of the device, the same electrodes were patterned onto an alumina substrate as well and similar measurements were made. In this section, the effect that the substrate has on the sensitivity will be investigated and discussed and how the dielectric constant of the substrate might affect the outcome of the results.

Measurements were taken with the same electrodes patterned on alumina substrates instead of silicon dioxide. The results showed that in most cases the sensitivity was increased when using the alumina substrates. However, the increase in the measured value did not have a common trend. In some cases the increase was as little as about 5% while some cases resulted in increases in sensitivity of up to 25%. In general though it can be seen that the substrate material does have some effect on the measurements and further study may be helpful in determining what the exact relationship is.

#### **4.2 Optimization of Sensor**

From what has been learned from the literature and from experiments, some rules about how to optimize this type of sensor have become apparent. First, a minimum spacing between the fingers of the interdigitated electrode is critical. It has been shown that the capacitance values measured and the sensitivity of the sensor is inversely proportional to the spacing. Second, the area of the sensor should be maximized. The overall width of the electrode and the thickness of

the fingers themselves will both come into play here. By making each large, the overall area of the sensor will be increased and thus increase the measurements taken and the sensitivity.

Further analysis of the data shows some other important information for optimization of the sensor. Each of the parameters will affect the sensitivity in varying amounts and will ultimately vary in the importance of design. From the data collected, the most important factor in increasing sensitivity is to increase the electrode width. By increasing the width of the electrode, the area is greatly increased and will lead to the largest increase in sensitivity of all the parameters. The next most important parameter to consider is the metallization ratio which takes into account both the finger thickness and finger spacing. As the metallization ratio is increased an increase in the capacitance will also be seen. The metallization ratio can be increased by either increasing finger thickness or decreasing finger spacing. Finally, the number of fingers is also important, however from the data it can be seen that a maximum sensitivity seems to be reached at 60 fingers so it leaves little to decide upon in a design. The fifth factor, substrate type, showed mixed results. However, the use of alumina most definitely had an effect on the measurements and generally caused the sensitivity to increase. Finding a better substrate may also prove useful once a suitable geometric design is established.

## CHAPTER 5

### CONCLUSIONS AND FUTURE STUDIES

An interdigitated electrode sensor was studied and optimized to be used as a sensor for detecting the dielectric properties of lubricant oils. The various design parameters were tested and the trends garnered from those experiments allowed for the optimization of capacitance measurements to be used as a basis for determining the quality of the oil. It was shown that by minimizing the spacing between the fingers of the interdigitated electrode and increasing the electrode area that greater resolution could be achieved. Furthermore, it was shown that the metallization ratio which includes both finger thickness and spacing was a major factor affecting the sensitivity. The number of fingers used in the electrode showed maximum sensitivity at 60 fingers. The effect of substrate material was also studied. The results showed that there was a noticeable effect but it was not constant.

A gap between the expected values that were generated using the mathematical IDC model of Igreja and Dias, and the measured value was observed. Several reasons for the gap and additions to the model were discussed. A large part of the gap seems to be due to the oxidation of the adhesion layer used to get the gold electrodes to adhere to the silicon dioxide substrate. The model did not take this into account originally and when it was added showed a definite increase in the model value for capacitance.

Future studies in this area should include the testing of several additional components to the degradation of oil. It has been shown that the inclusion of wear particles and moisture content will also affect the electrical properties of the oil as it degrades. The sensor should also be used to test how these variables affect the measurements taken by the sensor. The temperature of the sample should also be taken into consideration. Again, literature shows that the dielectric constant of oil is sensitive to temperature increase above 55 C. The sensor should be tested to see how the temperature affects its readings and where in the oil reservoir it can be successfully implemented. Finally, a threshold for when oil becomes unusable should be established and how the sensor responds at that point of degradation should be determined.

## REFERENCES

1. P.M. Mousavi, D. Wang, C.S. Grant, W. Oxenham, P.J. Hauser. Measuring Thermal Degradation of a Polyol Ester Lubricant in Liquid Phase. *Ind. Eng. Chem. Res.* 44 (2005) 5455 – 5464.
2. D. Wang, P. Mousavi, P.J. Hauser, W. Oxenham, C.S. Grant. Novel Testing System for Evaluating the Thermal Stability of Polyol Ester Lubricants. *Ind. Eng. Chem. Res.* 42 (2004) 6638 – 6646.
3. S.K. Naldu, E.E. Klaus, J.L. Duda. Kinetic model for high-temperature oxidation of lubricants. *Ind. Eng. Chem. Prod. Res. Dev.* 25 (1988) 596 – 603.
4. W.F. Bowman, G.W. Stachowiak. Determining the oxidation stability of lubricating oils using sealed capsule differential scanning calorimetry (SCDSC). *Tribology International* 29 (1996) 27 – 34.
5. S. Natarajan, W.W. Olson, M.A. Abraham. Reaction pathways and kinetics in the degradation of forging lubricants. *Ind. Eng. Chem. Res.* 39 (2000) 2837 – 2842.
6. D.L. Wooton. Applications of spectroscopy in the fuels and lubrication industry. *Applied Spectroscopy Reviews* 36 (2001) 315 – 332.
7. J.D. Turner, L. Austin. Electrical techniques for monitoring the condition of lubrication oil. *Meas. Sci. Technol.* **14** (2003) 1794 – 1800.

8. R.D. Lee, H.J. Kim, Y.P. Semenov. A coil type capacitive sensor for measurement of the deterioration of engine oil. CPEM Digest (Conference on Precision Electromagnetic Measurements) (2002) 184-185.
9. W.T. Kim, M.Y. Choi, H.W. Park, J.H. Park. Development of a coil-typed oil sensor system for the automobile engine oil on the dielectric constant.
10. S. Raadnui, S. Kleesuwan. Low-cost condition monitoring sensor for used oil analysis. Wear 259 (2005) 1502 – 1506.
11. M.A. Keller, C.S. Saba. Monitoring of ester base lubricants by dielectric constant. Lubrication Engineering 45 (1989) 347-351.
12. Y. Liu, X. Li, X. Cao. On-line monitoring system of vehicle lubricants quality based on the permittivity. Proceedings of the 2009 IEEE International Conference on Mechatronics and Automation. (2009) 2591-2595.
13. D. Yang, X. Zhang, Z. Hu, Y. Yang. Oil contamination monitoring based on dielectric constant measurement. 2009 International Conference on Measuring Technology and Mechatronics Automation. (2009) 249 – 252.
14. V.F. Lvovich, M.F. Smiechowski. Impedance characterization of industrial lubricants. Electrochimica Acta **51** (2006) 1487 – 1496.
15. S.S. Wang, H-S. Lee. The development of *in situ* electrochemical oil-condition sensors. Sensors and Actuators B **17** (1994) 179-185.
16. S.S. Wang. Road tests of oil condition sensor and sensing technique. Sensors and Actuators B 73 (2001) 106-111.
17. Y. Liu, Z. Liu, Y. Xie, Z. Yao. Research on an on-line wear condition monitoring system for marine diesel engine. Tribology International 33 (2000) 829 – 835.

18. S.S. Wang. Engine oil condition sensor: method for establishing correlation with total acid number. *Sensors and Actuators B* 86 (2002) 122 – 126.
19. P.A. Lieberzeit, G. Glanznig, A. Leidl, H. Nannen, F.L. Dickert. Nanostructured functional polymers for engine oil quality sensors. *IEEE* (2004) 449 – 450.
20. DTI Technology Group: Automotive Components. Oil Quality Sensors. Delphi Inc.
21. J. Min, A.J. Baeumner. Characterization and optimization of interdigitated ultramicroelectrode arrays as electrochemical biosensor transducers. *Electroanalysis* 16 (2004) 724 – 729.
22. R. Igreja, C.J. Dias. Analytical evaluation of the interdigital electrodes capacitance for a multi-layered structure. *Sensors and Actuators A* 112 (2004) 291 – 301.
23. J. Lin, S. Moller, E. Obermeier. Two-dimensional and three-dimensional interdigital capacitors as basic elements for chemical sensors. *Sensors and Actuators B* 5 (1991) 223-226.
24. D. Caratelli, R. Cicchetti. A full-wave analysis of interdigital capacitors for planar integrated circuits. *IEEE Transactions on Magnetics* 39 (2003) 1598 – 1601
25. K. Kim, M.S. Ahn, J.H. Kang, I. Yun. Circuit modeling of interdigitated capacitors fabricated by high-K LTCC sheets. *ETRI Journal* 28 (2006) 182 – 190.
26. P.M. Harrey, P.S.A. Evans, B.J. Ramsey, D.J. Harrison. Interdigitated capacitors by offset lithography. *Journal of Electronics Manufacturing* 10 (2000) 69 – 77.
27. J.L. Hobdell. Optimization of interdigital capacitors. *IEEE Transactions on Microwave Theory and Techniques* 27 (1979) 788 – 791.
28. H.E. Endres, S. Drost. Optimization of the geometry of gas-sensitive interdigital capacitors. *Sensors and Actuators B* 4 (1991) 95 – 98.

29. J. Laconte, V. Wilmart, D. Flandre, J.-P. Raskin. High-sensitivity capacitive humidity sensor using 3-layer patterned polyimide sensing film. *IEEE* (2003) 372 – 377.
30. N. Dib, J. Ababneh, A. Omar. CAD modeling of coplanar waveguide interdigital capacitor. *Int. J RF and Microwave CAE* 15 (2005) 551 – 559.
31. F.P. Casares-Miranda, P. Otero, E. Marquez-Segura, C. Camacho-Penalosa. Wire bonded interdigital capacitor. *IEEE Microwave and Wireless Components Letters* 15 (2005) 700 – 702.
32. A.P. Washabaugh, A. Mamishev, Y. Du, M. Zahn. Dielectric Measurements of semi-insulating liquids and solids. Conference Record of the ICDL '96 12<sup>th</sup> International Conference on Conduction and Breakdown in Dielectric Liquids (1996) 381 – 384.
33. N.J. Kidner, A. Meier, Z.J. Homrighaus, B.W. Wessels, T.O. Mason, E.J. Garboczi. Complex electrical (impedance/dielectric) properties of electroceramic thin films by impedance spectroscopy with interdigital electrodes. *Thin Solid Films* 515 (2007) 4588 – 4595.
34. E. Marquez-Segura, F.P. Casares-Miranda, P. Otero, C. Camacho-Penalosa, J.E. Page. Analytical model of the wire-bonded interdigital capacitor. *IEEE Transactions on Microwave Theory and Techniques* 54 (2006) 748 – 754.
35. Air BP Lubricants. BP Turbo Oil 2380 Product Data Sheet.
36. J. Li. Development of a microfabricated sensor array for oil evaluation. Dissertation, Case Western Reserve University (2005)
37. W. Zhang, J.R. Smith. Nonstoichiometric interfaces and Al<sub>2</sub>O<sub>3</sub> adhesion with Al and Ag. *Physical Review Letters* 85 (2000) 3225 - 3228.

38. M. Voigt, M. Sokolowski. Electrical properties of thin rf sputtered aluminum oxide films. *Materials Science and Engineering B* 109 (2004) 99 – 103.
39. C.S. Bhatia, G. Guthmiller, A.M. Spool. Alumina films by sputter deposition with Ar/O<sub>2</sub>: Preparation and characterization. *J. Vac. Sci. Technol. A* 7 (1989) 1298 – 1302.
40. B.G. Segda, M. Jacquet, J.P. Besse. Elaboration, characterization and dielectric properties study of amorphous alumina thin films deposited by r.f. magnetron sputtering. *Vacuum* 62 (2001) 27 – 38.
41. H. Birey. Dielectric properties of aluminum oxide films. *J. Appl. Phys.* 49 (1978) 2898 – 2904.
42. P. Katiyar, C. Jin, R.J. Narayan. Electrical properties of amorphous aluminum oxide thin films. *Acta Materialia* 53 (2005) 2617 – 2622.
43. T.P. Nguyen, J. Ip, P. Le Rendu, A. Lahmar. Improved Adhesion of gold coatings on ceramic substrates by thermal treatment. *Surface and Coatings Technology* 141 (2001) 108 – 114.
44. R. Igreja, C.J. Dias. Analytical evaluation of the interdigital electrodes capacitance for a multi-layered structure. *Sensors and Actuators A* 112 (2004) 291-301.